Gondwana Research 27 (2015) 486–506

Contents lists available at ScienceDirect

Gondwana Research

journal homepage: www.elsevier.com/locate/gr

The origin and significance of crustal minerals in ophiolitic chromitites and peridotites

Paul T. Robinson [a,*], Robert B. Trumbull [b], Axel Schmitt [c], Jing-Sui Yang [a], Jian-Wei Li [d], Mei-Fu Zhou [e], Jörg Erzinger [b], Sarah Dare [f], Fahui Xiong [a]

[a] CARMA, Key Laboratory for Continental Tectonics and Dynamics, Institute of Geology, Chinese Academy of Geological Sciences, Beijing 100037, China
[b] Helmholtz Centre Potsdam, Telegrafenberg, D-14473 Potsdam, Germany
[c] Department of Earth and Space Sciences, University of California, Los Angeles, Los Angeles, CA 90095-1567, USA
[d] Faculty of Earth Resources, China University of Geosciences, Wuhan 430074, China
[e] Department of Earth Sciences, The University of Hong Kong, Pokfulam, Hong Kong
[f] Department of Applied Sciences, University of Quebec at Chicoutimi, Saguenay, Canada

ARTICLE INFO

Article history:
Received 17 December 2013
Received in revised form 4 June 2014
Accepted 5 June 2014
Available online 26 June 2014

Keywords:
Podiform chromitite
Zircon
SIMS geochronology
Oman
Tibet
Polar Urals

ABSTRACT

Various combinations of zircon, quartz, corundum, K-feldspar, plagioclase, apatite, amphibole, rutile, titanite, almandine garnet, kyanite, andalusite, and coesite have been recovered from podiform chromitites of the Luobusa and Dongqiao ophiolites in Tibet, the Oman ophiolite and the Ray–Iz ophiolite in the Polar Urals, Russia. Chromitites in all four ophiolites also contain moissanite and the Luobusa and Ray–Iz ophiolites contain in-situ diamonds. Most of the recovered zircons are sub-rounded grains with complex internal structures indicating polyphase growth. Trace element contents and a low-pressure inclusion assemblage (quartz, muscovite, K-feldspar, apatite, ilmenite, rutile) indicate a continental crustal origin for the zircons. They have SIMS U–Pb ages that are generally much older than the host body (total range: 90 to 2500 Ma). The presence of numerous crustal minerals, particularly zircon, suggests derivation from metasedimentary rocks subducted into the mantle. Their preservation in chromitites and peridotites implies effective isolation from the mafic melts that formed the ophiolites. We suggest that most of these minerals were derived from the crustal parts of subducted slabs and were encapsulated into chromite grains precipitated from rising asthenospheric and suprasubduction magmas. The chromite grains were carried in melt channels to shallow levels in suprasubduction mantle wedges and then deposited as podiform chromitites near the Moho. The rise of asthenospheric peridotites into suprasubduction zones was facilitated by subduction initiation and possibly by slab tear allowing mixing of the UHP, highly reduced minerals and crustal minerals now found in ophiolitic chromitites and peridotites.

1. Introduction

Seismic tomography indicates that crustal slabs are subducted to mantle depths but the fate of this material is still unclear. In continental collision zones such as the Dabie–Sulu orogen of China, deeply subducted crust is subjected to ultrahigh-pressure (UHP) metamorphism at depths in excess of 100 km and then rapidly exhumed (Liu et al., 2004). These metamorphic rocks are chiefly gneisses and eclogites that contain both high- and ultrahigh-pressure minerals. Their UHP metamorphism is clearly recorded by the presence of diamond and coesite as inclusions in zircon and garnet. Commonly, the zircons from these rocks are complexly zoned with old, inherited cores surrounded by overgrowths of younger age (Katayama et al., 2001). Typically, the older cores have Proterozoic ages and contain inclusions of low-pressure crustal minerals, such as quartz, K-feldspar, plagioclase, apatite and mica whereas the UHP minerals are hosted in mantles or rims surrounding the cores. In some cases, however, UHP inherited cores with coesite, phengite and apatite are surrounded by younger magmatic rims containing inclusions of quartz, K-feldspar, albite and apatite, interpreted as the products of partial melting during exhumation (Liu et al., 2002, 2007).

Although UHP metamorphic belts provide evidence for rapid exhumation of deeply subducted crust, seismic tomography indicates that lithospheric slabs can descend at least to the mantle transition zone (e.g., van der Hilst, 1995) and there is abundant geochemical evidence for a crustal contribution to different reservoirs in the mantle (e.g. Hoffmann, 1997). Thus, it appears that significant amounts of crustal material can be added to the mantle reservoir, but when and how it is incorporated is not clear.

During an on-going study of UHP and related minerals in podiform chromitites (e.g., Bai et al., 2000; Robinson et al., 2004; Yang et al., 2007; Trumbull et al., 2009), we have identified a variety of accessory crustal minerals including zircon, corundum, kyanite, andalusite, almandine garnet, quartz, K-feldspar, titanite and rutile in one or more of four ophiolites, Luobusa and Dongqiao in Tibet, the Oman ophiolite

* Corresponding author.
E-mail address: paulrobinson94@hotmail.com (P.T. Robinson).

http://dx.doi.org/10.1016/j.gr.2014.06.003
1342-937X/

Table 1
Crustal and other minerals identified in chromitites of the Loubusa, Dongqiao, Semail and Ray–Iz ophiolites.

Mineral	Luobusa	Dongqiao	Semail	Ray–Iz
Alm garnet	x		x	x
Andalusite	x			x
Amphibole	x		x	x
Apatite	x	x	x	x
Aragonite	x			
Biotite	x			
Brucite	x			
Coesite	x			x
Corundum	x	x	x	x
Diamond	x	x		x
Fluorite	x			
K-Feldspar	x	x	x	
Kyanite	x			x
Muscovite	x			
Moissanite	x	x	x	x
Plagioclase	x	x		x
Quartz	x	x	x	x
Rutile	x	x	x	x
Titanite	x		x	x
Topaz				x
Tourmaline	x			
Zircon	x	x	x	x

and the Ray–Iz ophiolite of the Polar Urals, Russia (Table 1). Here we use the term crustal minerals to include phases commonly found in crustal rocks, even though some might have crystallized in the mantle. The Luobusa and Ray–Iz chromitites also contain in-situ diamond and coesite, and all four ophiolites contain moissanite (SiC). Because the chromitites all lie within oceanic mantle peridotite, there was no opportunity for direct contamination by continental crust during their formation and great care was taken to avoid anthropogenic contamination during sample collection and mineral separation. Some of the minerals described here, such as diamond, moissanite, coesite, kyanite, and corundum, have also been found in-situ, hosted in chromite or olivine grains (Yang et al., 2015-in this issue). Thus, the discovery of similar crustal minerals from four widely separated ophiolites provides strong evidence for recycling of crustal components through the upper mantle.

In the current study, we focused on zircon from the four ophiolites because this mineral provides both compositional and geochronological evidence for the provenance of individual grains. However, we describe the other crustal minerals to show that such phases are common in oceanic chromitites and peridotites. Zircons were previously reported from the Luobusa ophiolite (e.g., Hu, 1999; Robinson et al., 2004) and some grains were found to be much older than the ophiolite (Yamamoto et al., 2004, 2013; Robinson et al., 2013). We confirm the presence of old zircons in Luobusa, but more importantly, we also show that this is not an isolated occurrence. Very similar collections of old zircon in chromitites of the Dongqiao and Oman ophiolites are reported in this paper. Most zircons in the Ray–Iz ophiolite are thought to have formed by mantle metasomatism, but a few grains of old zircon are also present (Savelieva et al., 2007).

2. Geological background

2.1. Luobusa ophiolite

The Luobusa ophiolite lies in the Yarlung–Zangbo suture zone in southern Tibet about 200 km ESE of Lhasa. It is a fault-bounded slab, 1–2 km thick, consisting chiefly of harzburgite and Cpx-bearing harzburgite (Fig. 1). It is thought to have originated at a mid-ocean ridge at ~177 Ma (Zhou et al., 2002) and then been modified by boninitic melts above an intraoceanic subduction zone at ~126 Ma (Zhou et al., 1996; Malpas et al., 2003; Zhou et al., 2005; Yamamoto et al., 2007). The harzburgites overlie a sequence of 'transition-zone' dunites believed to have been formed by extensive melt–rock reaction (Zhou et al., 2005). The ophiolite hosts numerous lenses, layers and pods of chromitite in the mantle harzburgite (Fig. 2a, b) where they are commonly surrounded by envelopes of dunite formed by melt–rock reaction in the upper mantle (Zhou et al., 1996, 2005). Our samples from orebodies 11 (Kangjinla district; 29°11.52′N; 92°17.73′E), 31 (Luobusa District; 29°10.23′N; 92°10.80′E) and 74 (Xiangkashan District; 29°11.40′N; 92°15.30′E) contain 80–90 vol.% chromite with Cr# (100 * Cr / Cr + Al) of 79–93 (Zhou et al., 1996). The Luobusa chromitites are well-known for the occurrence of ultrahigh-pressure and highly reduced minerals such as diamond, coesite, moissanite,

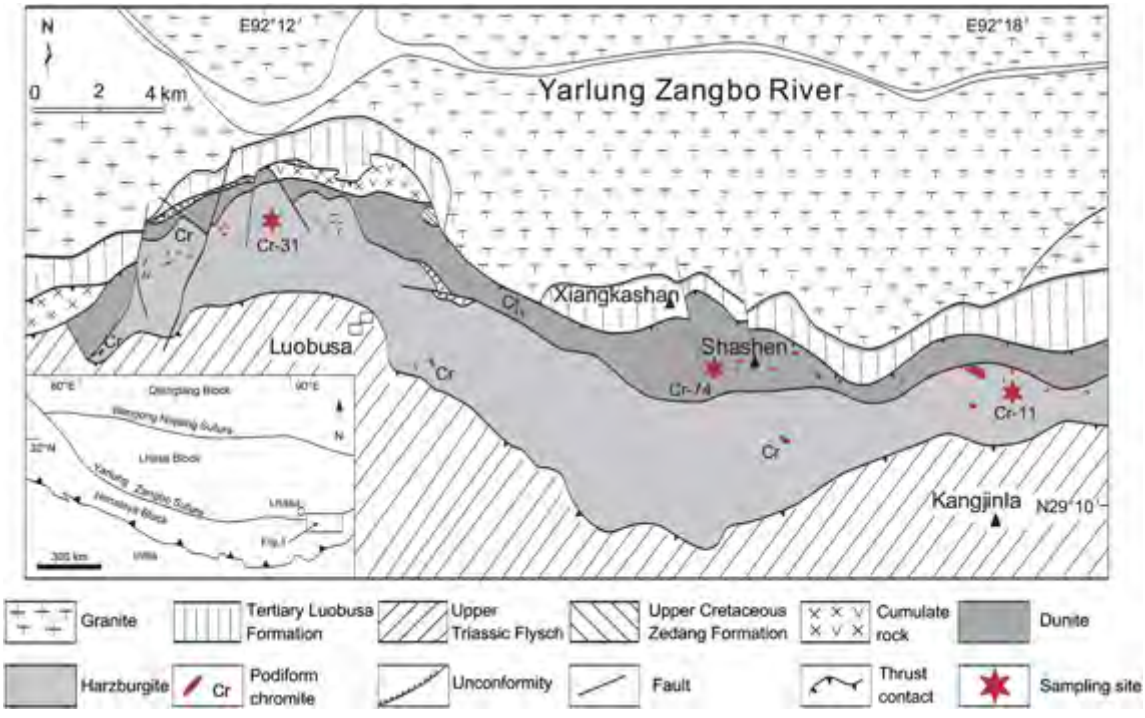

Fig. 1. Sketch map of the Luobusa ophiolite, Tibet showing sampling locations.

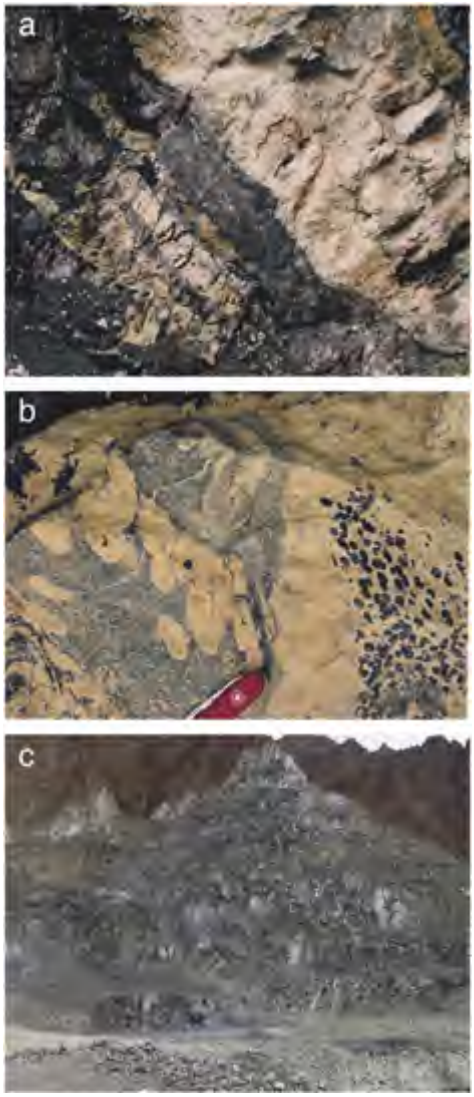

Fig. 2. Typical outcrops of podiform chromitites. a) Layers of massive chromitite hosted in harzburgite. The largest layer is about 1 m thick — orebody 31, Luobusa ophiolite; b) disseminated, nodular and massive chromitite in dunite — orebody 11, Luobusa ophiolite. Note the brittle fracturing of the dunite and intrusion of the disseminated chromitite; c) podiform body of massive chromitite about 30 m thick — Shamis 2 mine in Wadi Rajmi, Semail ophiolite, Oman.

FeSi alloys and numerous native elements (Fang and Bai, 1981; Bai et al., 2000, 2001; Robinson et al., 2004; Yang et al., 2007; Xu et al., 2009; Yang et al., 2014).

2.2. Dongqiao ophiolite

The Dongqiao ophiolite is located in the Bangong Lake-Nujiang suture zone in central Tibet (Fig. 3). It consists of an 18-km-long block of harzburgite hosting lenses and pods of chromitite with compositions similar to those of Luobusa (Cr# of 70–80: Shi et al., 2007). Amphiboles separated from the metamorphic sole have $^{40}Ar/^{39}Ar$ ages of 175–180 Ma (Zhou et al., 1997), suggesting formation in the Middle Jurassic. The bulk sample from which the minerals were separated originated from orebody Nr. 10 located at approximately 90°38.12′E; 32°01.00′ N.

2.3. Semail ophiolite

The Oman ophiolite in Oman and the United Arab Emirates (UAE) forms part of the Tethyan belt that extends from Europe through the Middle East to Tibet and beyond (e.g. Searle and Cox, 1999). Podiform chromitites occur both at the top of the mantle and deeper in the section (at least 6 km below the Moho; e.g., Ahmed and Arai, 2002; Rollinson, 2008). The chromite composition is variable in these bodies, generally being highest at the north end of the ophiolite in the UAE. Like the other ophiolites, these chromitite pods are associated with veins and envelopes of dunite. We collected samples from two localities in the ophiolite (Fig. 4). Sample OM-2, which is from the Shamis 2 orebody in Wadi Rajmi, Oman (24°36.34′N; 56°14.52′E), consists of massive chromitite (Fig. 2c) (Cr# = 64; Rollinson, 2008) with interstitial olivine and orthopyroxene, accompanied by minor clinopyroxene and amphibole. Sample UAE-1 (25°4.66′N; 56°13.41′E) is massive chromite ore with minor olivine taken from a 1- to 1.5-m-thick chromitite lens in harzburgite from a defunct mine in Wadi Al-Hayl.

2.4. Ray–Iz ophiolite

The Ray–Iz ophiolite occurs at the NE end of the Paleozoic Voikar-Syninsk ophiolite belt (Fig. 5) (Saveliev and Savelieva, 1977; Garuti et al., 1999; Yang et al., 2015-in this issue). A summary of age data for the ophiolite belt (Savelieva et al., 2007) indicates formation in the late Cambrian to early Ordovician. The Ray–Iz ophiolite crops out over ~400 km^2 and consists chiefly of upper mantle harzburgite and dunite, locally overlain by minor amounts of cumulate gabbro above the Moho. More than 200 podiform chromitite orebodies occur in the ophiolite, hosted chiefly in the harzburgite-dunite complex and consisting of high-Cr chromite (Cr# = 74–80) (Pervozhikov et al., 1990). Samples of chromitite were collected from two orebodies CCD (66°52.06′N; 65°15.72′E) and W214 (66°49.62′N; 65°07.45′E) (Fig. 5).

3. Origin of podiform chromitites

Two basic types of chromitite are recognized; stratiform and podiform (Thayer, 1960, 1964). Here we distinguish between chromite (individual grains) and chromitite (bodies and layers of aggregated chromite). Stratiform chromitites occur as relatively thin layers of massive chromite with a wide areal extent, interlayered with mafic and ultramafic cumulates in large bodies such as the Stillwater, Muskox, and Bushveld intrusions (e.g., Irvine, 1977). Based on their textures and occurrence within layered sequences they are interpreted as cumulate layers precipitated from mafic magmas, although the processes by which such vast amounts of chromite are extracted from mafic magmas are still not clear. The large mafic intrusions hosting stratiform chromitites occur exclusively in stable cratonic areas.

Podiform chromitites, in contrast, are relatively small, tabular to lenticular, bodies of chromite (Fig. 2) hosted chiefly in the mantle sections of ophiolites, although some small chromitites may also occur in the overlying cumulate sequences. Most extend for less than 100 m along strike and rarely exceed 50 m in thickness. Unlike stratiform chromitites, these bodies display a wide range of textures ranging from layered, massive, and disseminated to nodular and antinodular (Thayer, 1964) (Fig. 2). Podiform chromitites are typically hosted in mantle harzburgites, or less commonly in lherzolites, and are characteristically associated with small pods, veins and envelopes of dunite. Detailed studies of these dunites indicate that they are products of melt–rock reaction during which orthopyroxene is dissolved and olivine is precipitated (Kelemen, 1990; Kelemen et al., 1992; Zhou et al., 1996). The chromian content of the chromitites is generally thought to be related to the composition of the parental magma, with Cr-rich bodies having been derived from boninitic melts and more aluminous bodies from MORB-like or arc tholeiite magmas (Zhou et al., 1996). However, it is clear that chromite compositions can also be modified by melt–rock reaction (e.g., Zhou et al., 1996). In some ophiolites, the Cr# of chromitites varies spatially (Ahmed and Arai, 2002) and vertically (Rollinson, 2008) in the mantle section. In addition, some ophiolites contain both high-Cr and high-Al chromitites in the same peridotite body (Xiong et al., 2015-in this issue).

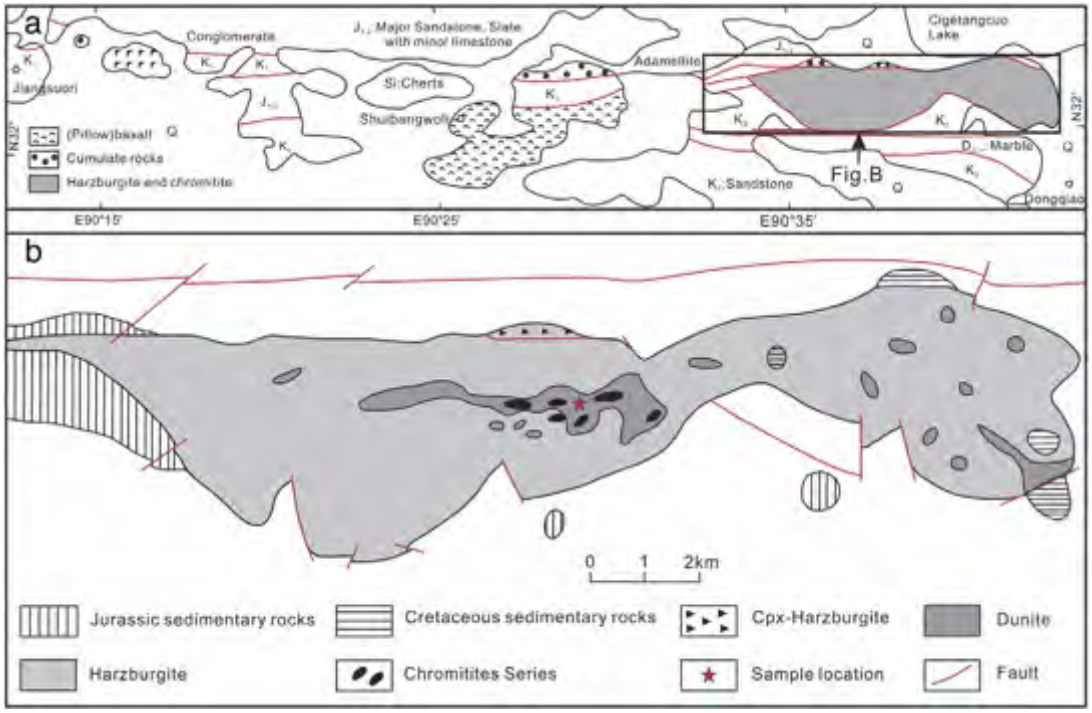

Fig. 3. Sketch geologic map of the Dongqiao ophiolite, Tibet showing sampling location. Modified from Shi et al., 2012.

On the basis of their textures, the compositions of their host rocks and their association with dunite, podiform chromitites are thought to form at shallow levels in the mantle by precipitation from mafic melts passing through, reacting with and ponding in the host peridotites (Zhou and Robinson, 1994; Zhou et al., 1996; Zhou and Robinson, 1997; Rollinson and Adetunji;, 2013). However, the occurrence of diamond and coesite in the Luobusa and Ray–Iz chromitites (Yang et al., 2007, 2015-in this issue) and the discovery of coesite exsolution lamellae in chromite grains from Luobusa (Yamamoto et al., 2009) challenge some aspects of that view. It is difficult to escape the conclusion that at least some of the chromite in the Luobusa and Ray–Iz ophiolites crystallized at depth, although the textures and field relationships leave little doubt that many of the chromitites were formed at a shallow mantle level (perhaps a few kilometers below the MOHO). Such an interpretation is strongly supported by the occurrence of podiform chromitites in the Troodos and Semail ophiolites where their positions relative to the Moho can be easily established (Malpas and Robinson, 1987; Rollinson, 2008).

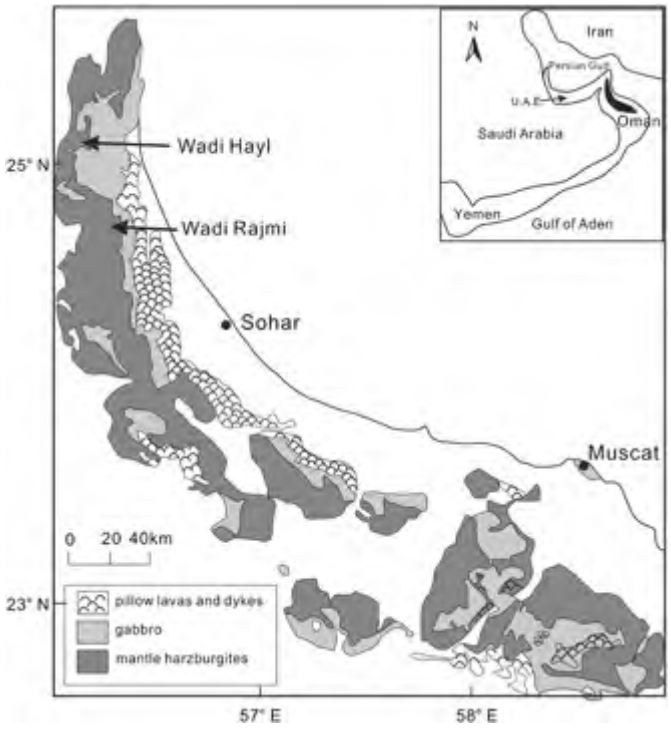

Fig. 4. Sketch geologic map of the Semail ophiolite, Oman, showing sampling locations. Modified from Rollinson, 2008.

4. The question of contamination

Because the UHP, highly reduced and crustal minerals reported from the various ophiolites are so unexpected there is always concern about possible natural or anthropogenic contamination of the samples. All of the minerals reported here occur in small quantities, requiring separation from between 100 and 500 kg of the host rock. For example, at Luobusa a 1000-kg sample of chromitite from Orebody 11 yielded approximately 1000 grains of diamond (Xu et al., 2011), a much higher recovery than most samples. However, in-situ grains of diamond (Yang et al., 2014), moissanite (Yang et al., 2014, 2015-in this issue) and corundum (Yang et al., 2015-in this issue) provide assurance that these minerals are inherent to the chromitites and peridotites. In addition, intergrowths of coesite and kyanite rimming a grain of FeTi alloy (Yang et al., 2007) are not compatible with a crustal formation. Numerous precautions were taken to minimize any chance of contamination (see Appendix I for details on sampling and separation procedures as well as analytical techniques). We carried out mineral separation in 3 different laboratories and obtained essentially the same results. Equally important, zircons have been reported independently by Yamamoto et al. (2013) from the Luobusa chromitites and by Lönngren and Kojonen (2005) and Savelieva et al. (2007) from the Ray–Iz chromitites. Thus, the in-situ grains and the recovery of the same minerals by independent workers from two of the ophiolites that we investigated clearly

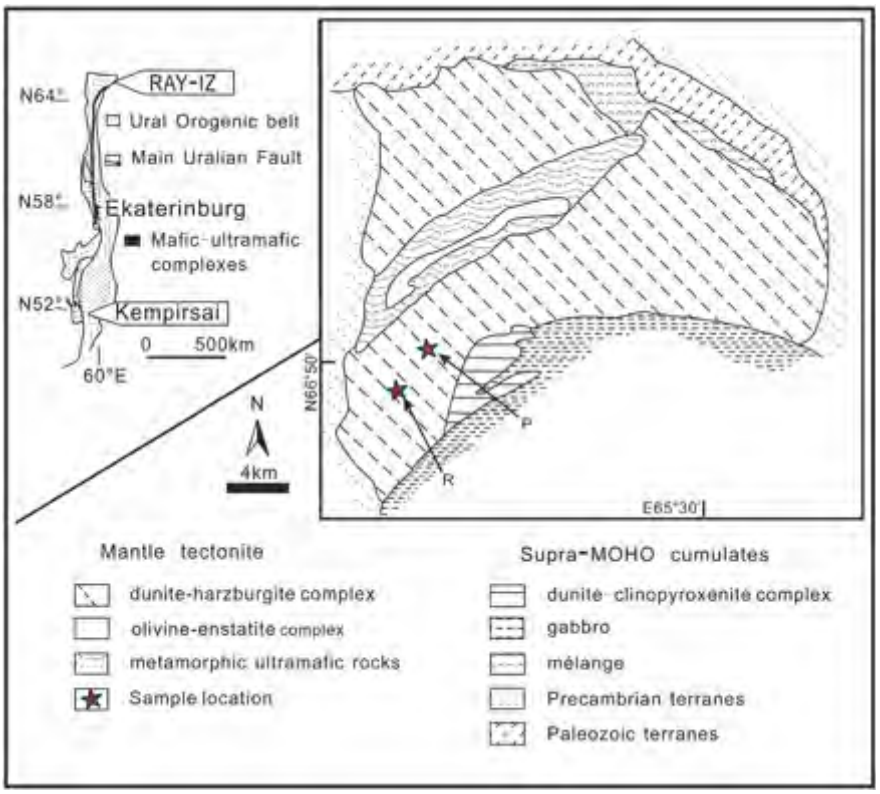

Fig. 5. Sketch geologic map of the Ray–Iz ophiolite, Polar Urals, Russia showing sampling locations. Modified from Schmelev and Meng, 2013.

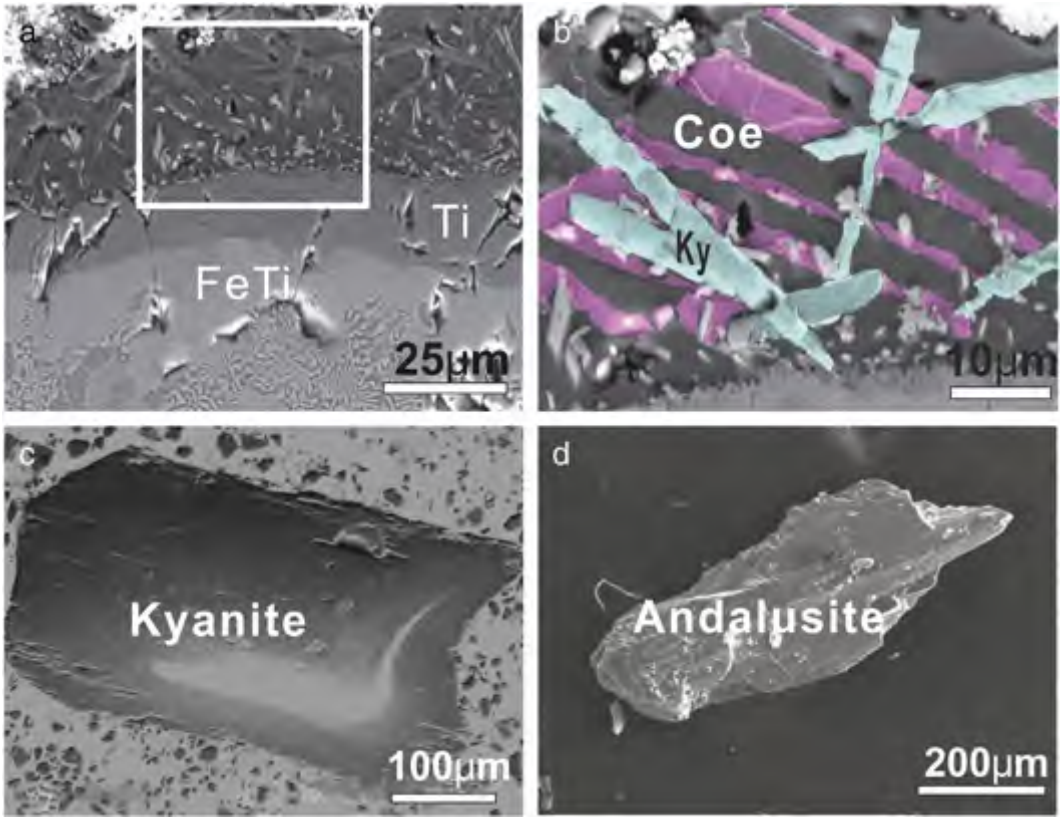

Fig. 6. Photographs of kyanite and coesite from podiform chromitites. a) Small grain of Fe–Ti alloy rimmed by a narrow band of native Ti, which in turn is rimmed with an intergrowth of coesite, kyanite and amorphous silicate; b) enlarged view of the square area shown in (a). Tabular crystals of coesite (coe) are intergrown with an amorphous silicate (pink color) and both are crosscut by tabular crystals of kyanite (ky). The form of the coesite suggests that it has pseudomorphically replaced stishovite (see Yang et al., 2007); c) tabular grain of kyanite recovered from chromitite of the Ray–Iz ophiolite, Russia; d) tabular grain of andalusite recovered from chromitite of the Luobusa ophiolite (Xu et al., 2009).

demonstrate that the minerals are naturally occurring grains from the host chromitites and peridotites. The in-situ minerals suggest that they were preserved by encapsulation in chromite grains.

5. Mineral descriptions

Chromitites from the Luobusa and Ray–Iz ophiolite have very similar collections of crustal minerals, whereas the Dongqiao and Oman ophiolites have a more limited assortment (Table 1). SEM images of representative minerals are shown in Figs. 6–14 and analyses of selected grains are presented in Tables 2–6.

5.1. Coesite and kyanite

Coesite and kyanite form an intergrown assemblage rimming a grain of FeTi alloy (Fig. 6a, b) recovered from chromitite orebody 31 of the

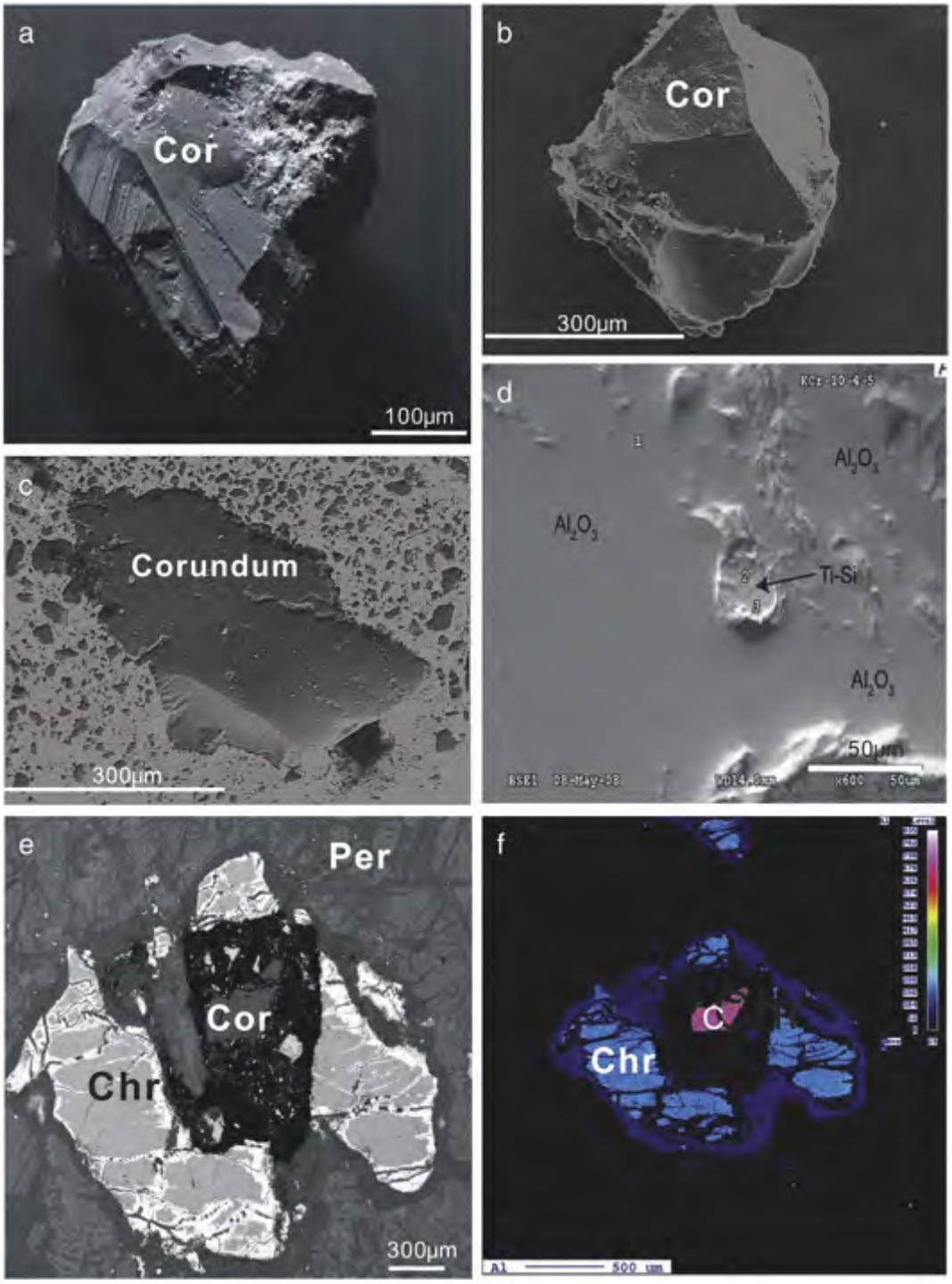

Fig. 7. SEM photographs of corundum grains recovered from podiform chromitite and peridotite. a) Blocky grain of corundum from the Shamis 2 mine of the Semail ophiolite showing growth zoning; b) angular grain of corundum from chromitite of the Ray–Iz ophiolite; c) angular fragment of corundum; d) inclusion of Ti–Si alloy in grain of corundum (KCr-10-4, Luobusa ophiolite); e) in-situ grain of corundum (Cor) in peridotite (Per) of the Luobusa ophiolite. The corundum grain is enclosed in a small patch of amorphous carbon (black), partly surrounded by chromite (chr); f) Al element map of (e) showing the corundum grain (pink) and the rimming chromite.

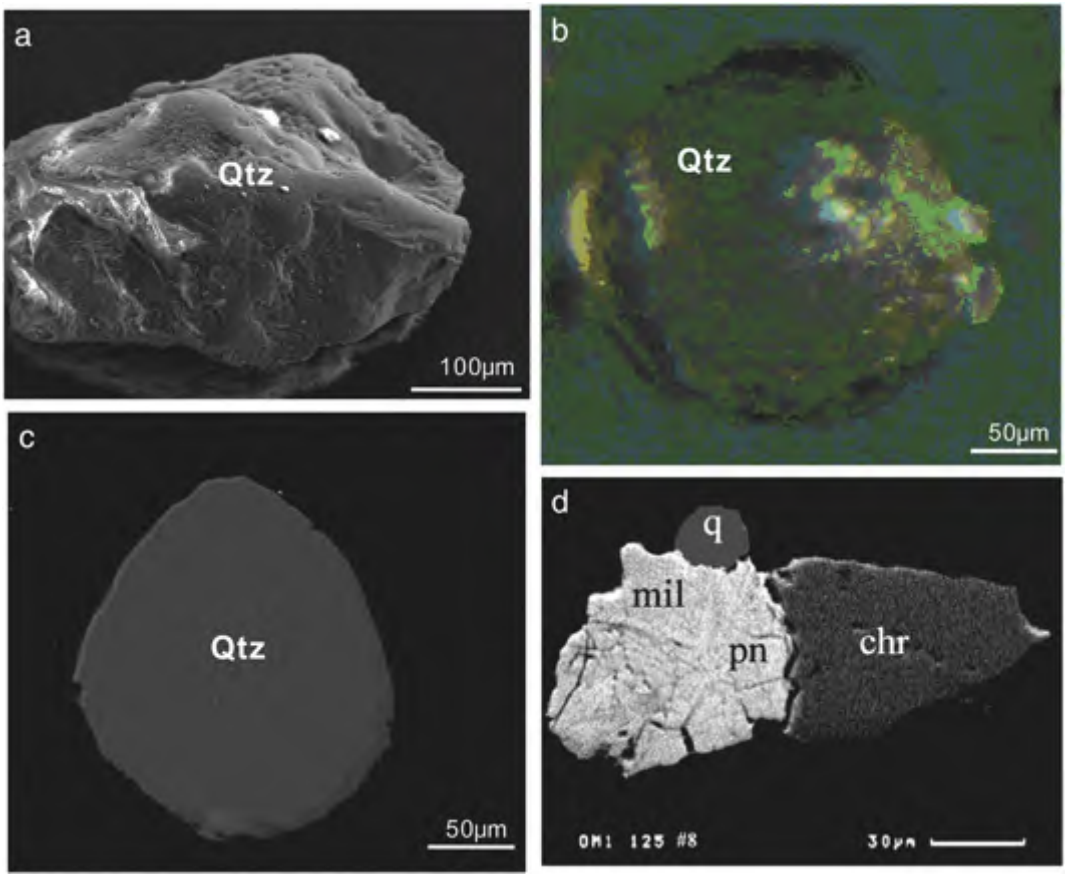

Fig. 8. Pictures of quartz grains recovered from podiform chromitites. a) SEM photograph of a relatively large, somewhat rounded quartz grain from the Shamis 2 mine, Semail ophiolite; b) photomicrograph of a rounded quartz grain from chromitite of the Luobusa ophiolite; c) SEM photograph of the grain in (b); d) SEM photograph of a small, angular quartz grain (q) attached to sulfide (millerite and pentlandite), which in turn, is attached to chromite from the Shamis 2 mine of the Semail ophiolite. The sulfide and quartz could be part of a vein or crack filling, although sulfides are very common in the chromitite.

Luobusa ophiolite (Yang et al., 2007). The coesite–kyanite intergrowth is separated from the TiFe alloy by a narrow band of native Ti (Fig. 6a). The coesite forms tabular crystals about 70–80 μm long and 5–8 μm wide intergrown with an unidentified, amorphous silicate with about 65 wt.% SiO_2. The shape of the coesite crystals and their crystallographic orientation strongly imply that they are pseudomorphs after stishovite (Yang et al., 2007), suggesting a depth of crystallization of roughly 300 km. Superimposed on this assemblage are tabular crystals of kyanite about 15–40 μm long and 5 μm wide, oriented at a high angle to the coesite grains. The textural relationships of this assemblage indicate that the coesite and kyanite grew in the mantle probably by a reaction between the TiFe alloy and previously subducted silicate material. The coesite consists of pure SiO_2, whereas the kyanite contains up to 2 wt.% TiO_2 (Table 2, column 1). A deep mantle origin is supported by the presence of minute grains of BN, a new mineral named qingsonite, between the coesite crystals (Dobrzhinetskaya et al., 2009).

A few grains of kyanite have also been recovered from the Ray–Iz ophiolite. These are irregular, tabular grains about 500 μm long and 200 μm wide (Fig. 6c). They have been identified by EDS analysis and single-crystal X-ray diffraction, and consist of 58.6 wt.% Al_2O_3 and 41.4 wt.% SiO_2. Small quantities of both andalusite and sillimanite have also been reported from the Luobusa chromitites. The sillimanite, identified only on the basis of microprobe analyses, forms white crystals about 1.5 mm long and 0.2 mm wide (Table 2, column 3) (Hu, 1999). Angular fragments of andalusite, about 500 μm long and 150 μm wide, have been identified by both microprobe (Table 2, column 4) and X-ray diffraction studies (Xu et al., 2009).

5.2. Corundum

Corundum is present in all of the chromitites examined. It occurs as blocky to sub-rounded, colorless to pink or blue grains or broken fragments, up to about 500 μm across (Fig. 7a–c). Although some grains show apparent growth patterns in SEM photographs (Fig. 7a), they consist of nearly pure Al_2O_3 with up to 2 wt.% TiO_2 and trace amounts of MgO and SiO_2 (Table 2). Some of the grains contain small inclusions, including grains of TiSi, up to about 25 μm across (Fig. 7d), with an average composition of 64.2 wt.% Si and 35.8 wt.% Ti (Xu et al., 2009). The presence of these inclusions suggests that the corundum was either crystallized or partly recrystallized under relatively deep mantle conditions. A deep mantle origin is also indicated by the presence of a corundum inclusion in an OsIr alloy from the Luobusa ophiolite (Bai et al., 2007).

Corundum has also been found in-situ in peridotite from Luobusa (Fig. 7e, f). This is a small grain about 300 μm across, with crystal faces preserved. It is embedded in a patch of amorphous carbon, which in turn, lies within a chromite grain surrounded by olivine and pyroxene. This mode of occurrence is similar to that of the in-situ diamonds, which are contained in mostly circular patches of amorphous carbon within chromite grains.

5.3. Quartz and moissanite

A few grains of quartz were recovered from all of the chromitites. Some grains are relatively large (up to 500 μm) and abraded (Fig. 8a); others are round (Fig. 8b, c) or subangular to irregular fragments. One grain recovered from Luobusa is attached to a sulfide, which in turn is

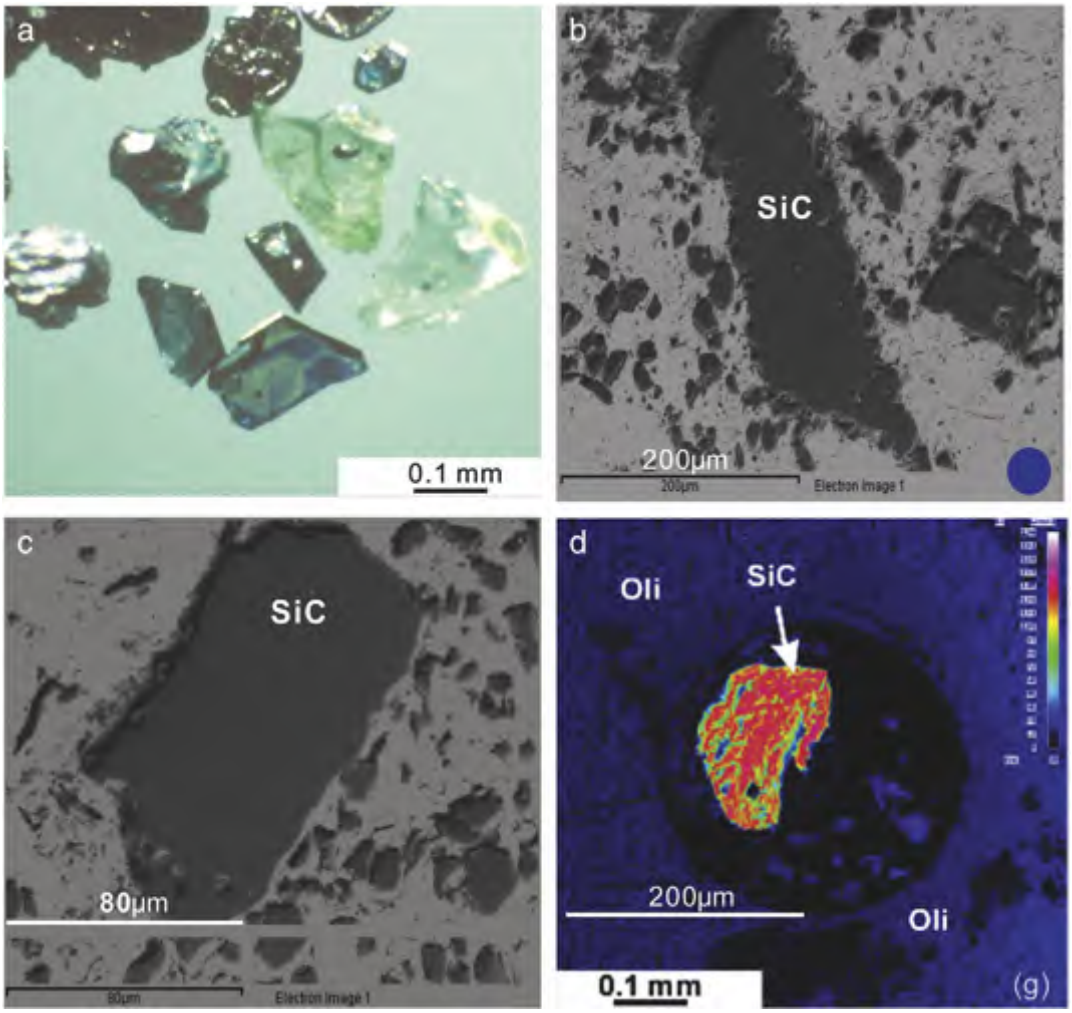

Fig. 9. Examples of moissanite from podiform chromitites of the Semail and Ray–Iz ophiolites. a) Photomicrograph of broken fragments of moissanite from the Shamis mine, Semail ophiolite — note partial hexagonal crystal faces; b, c) SEM images of moissanite from chromitites of the Ray–Iz ophiolite; d) carbon element map of an in-situ grain of moissanite enclosed in a circular patch of amorphous carbon (black area), hosted in peridotite of the Luobusa ophiolite. Note the partial hexagonal shape of the moissanite grain (reddish orange).

attached to a grain of chromite (Fig. 8d). The sulfide and quartz grain could represent a late-stage vein filling in the chromitite or they could be original grains. The analyzed quartz grains consist chiefly of SiO_2 (Table 3), although some have trace amounts of FeO.

Although moissanite (SiC) is not considered a crustal mineral, it is included here because of it occurs in all of the ophiolites investigated and one grain has been found in situ. It typically occurs as broken fragments of glassy, transparent to translucent crystals, generally 100–200 µm across. Some grains appear to be fragments of hexagonal crystals (lowest grain in Fig. 9a); others are irregular to tabular grains (Fig. 9b, c). The grains range from colorless, to light green to dark greenish-blue, making them easy to recognize. Some grains contain minute inclusions of FeSi or native Si and all analyzed grains have low C isotopes in a similar range as the diamonds (Trumbull et al., 2009).

One in-situ crystal of moissanite has been found in peridotite of the Luobusa ophiolite (Fig. 9d). It is about 200 µm across and appears to be half of a hexagonal crystal. The grain is hosted in a circular (spherical?) patch of amorphous carbon, similar to those hosting the in-situ diamonds in the chromitites (Yang et al., 2014). In this case, the patch of amorphous carbon is hosted in olivine, not chromite. The analyzed moissanite grains consist of almost pure SiC, although a few grains have trace amounts of FeO (Table 3). The relative abundance of moissanite in these rocks, its euhedral form and its in-situ occurrence confirm that it is not an industrial contaminant.

5.4. Garnet

Garnet was recovered from the Luobusa, Oman and Ray–Iz chromitites. Ir mostly forms reddish-brown, subhedral grains or broken fragments up to about 200 µm in size (Fig. 10). Some grains are blocky and angular but others have well-developed crystal faces. Most are Fe-rich almandine but some grains contain significant amounts of MnO. A few grains with up to 28 wt.% MnO (Table 4) are classified as spessartine. Interestingly, other Mn-rich phases are quite common in the ophiolitic chromitites, particular as Ni–Mn–Co alloys and other Mn-rich silicate minerals (Yang et al., 2014).

Rare grains of greenish uvarovite have also been recovered from both the Oman and Luobusa chromitites (Table 4).

5.5. Rutile, titanite, apatite, biotite, hornblende and feldspar

Rutile is relatively common in all of the chromitites (Table 1). It occurs as deep red, vitreous, round to elongate grains up to about 200 µm in length (Figs. 11a; 12a, c). Some grains host inclusions of zircon and apatite, which are 10–50 µm across (Fig. 12b, c). Most grains consist

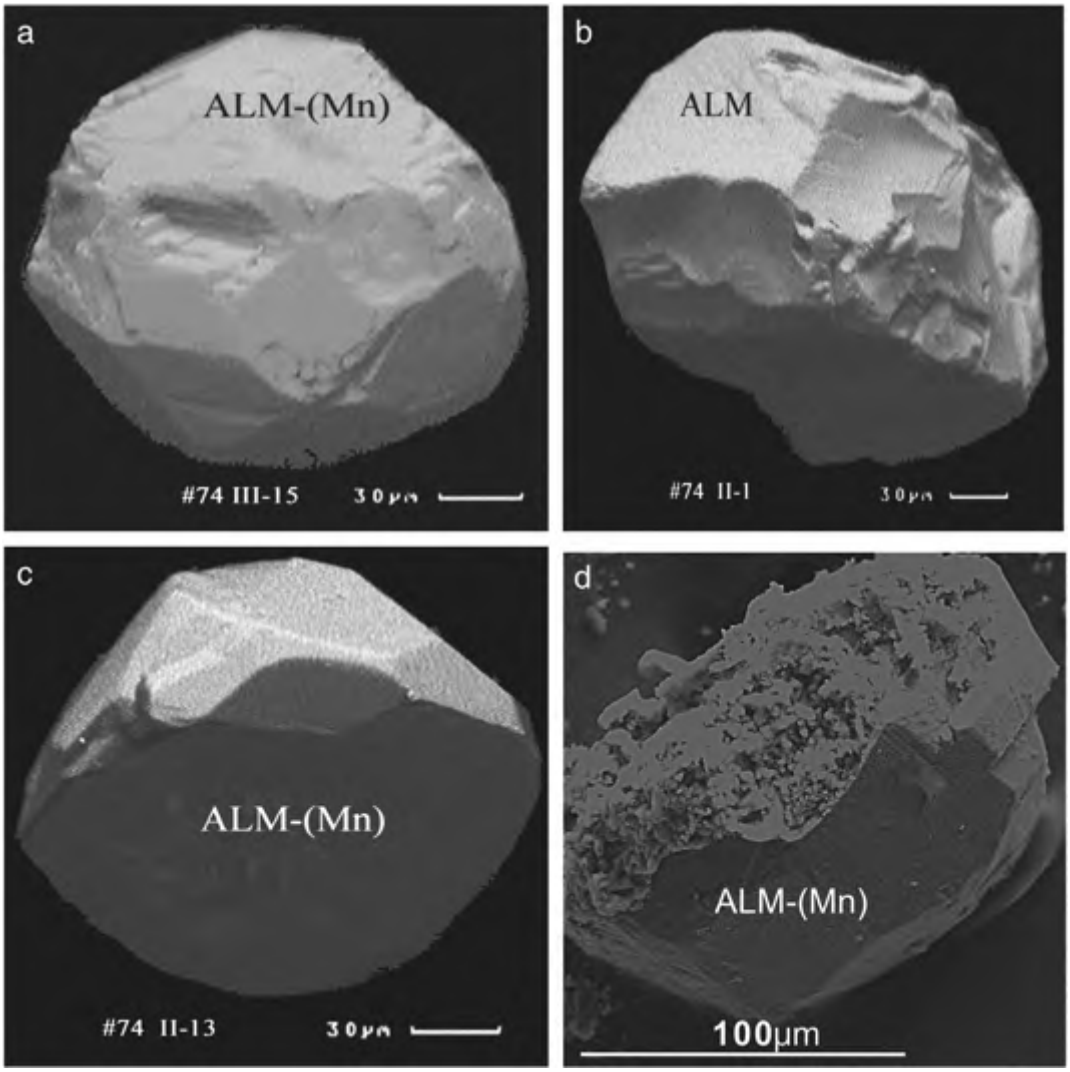

Fig. 10. SEM photographs of almandine garnet from the Luobusa and Ray–Iz ophiolites. a) Slightly rounded grain of MnO-bearing almandine garnet. Note poorly preserved crystal faces; b) broken grain of almandine garnet; c) grain of MnO-bearing almandine garnet with well-preserved crystal faces; d) broken fragment of MnO-bearing almandine garnet showing corrosion on the broken surface. Grains a, b, and c are from the Luobusa ophiolite and d is from the Ray–Iz ophiolite. All are from chromitites.

of essentially pure TiO_2 with traces of FeO, CaO and Al_2O (Table 5). One grain (KCr-11) has an inclusion of Ti_2O_3 (Fig. 11a) (Table 5). Grain R20-4 from the Ray–Iz ophiolite (not shown) has a small, round inclusion of quartz about 20 μm across.

Titanite was found in all but the Dongqiao chromitite. It forms elongate, somewhat rounded grains, 150–200 μm long and about 80 μm wide (Fig. 11b). It is relatively uniform in composition regardless of its source (Table 5).

Apatite typically forms white, angular grains up to about 30 μm across (Fig. 11c). It commonly also occurs as small, euhedral to subhedral inclusions, particularly in rutile where it is associated with zircon (Fig. 12b). It is relatively uniform in composition, consisting chiefly of CaO and P_2O_5 with very minor amounts of TiO_2, FeO, MnO, MgO and Na_2O (Table 5).

Small grains of amphibole have been recovered from all of the studied ophiolites except Dongqiao. Most grains are ragged prisms less than 100 μm in length (Fig. 11e). A typical composition of a grain from Luobusa is given in Table 5. Amphibole inclusions are common in chromitites from many different ophiolites and the presence of these hydrous phases is taken as strong evidence for the formation of ophiolites and chromitites in suprasubduction zone mantle wedges (e.g., Rollinson and Adetunji, 2013).

Rare flakes of biotite, phlogopite and even muscovite have also been recovered from the Luobusa and Oman ophiolite (Fig. 11e). The biotite and phlogopite occur as small, black plates a few tens of microns across. An analysis of a biotite grain is given in Table 5.

Very rare grains of tourmaline are present in the Luobusa chromites and one grain of topaz (Fig. 11d) was recovered from the Ray–Iz ophiolite. One grain of tourmaline contains a small inclusion of zircon.

5.6. Feldspar

Both plagioclase and orthoclase are present, albeit rare, in all four ophiolites. Plagioclase forms irregular laths, some of which occur in-situ (Fig. 11f). All of the analyzed plagioclase grains from the Luobusa ophiolite are relatively sodic (An_{28-50}), indicating a felsic source (Table 6). K-feldspar in Luobusa (Or_{85-98}) forms colorless, angular fragments up to 0.6 mm across, whereas that in the Dongqiao and Oman ophiolites occurs as subangular to rounded grains smaller than 100 μm. All of the grains are relatively uniform in composition (Table 6) and are probably orthoclase. Like the plagioclase, they indicate a felsic source.

5.7. Zircon

Zircon is present in all the ophiolites we investigated. In Luobusa, Dongqiao and Oman, it occurs chiefly as light brown, subangular to

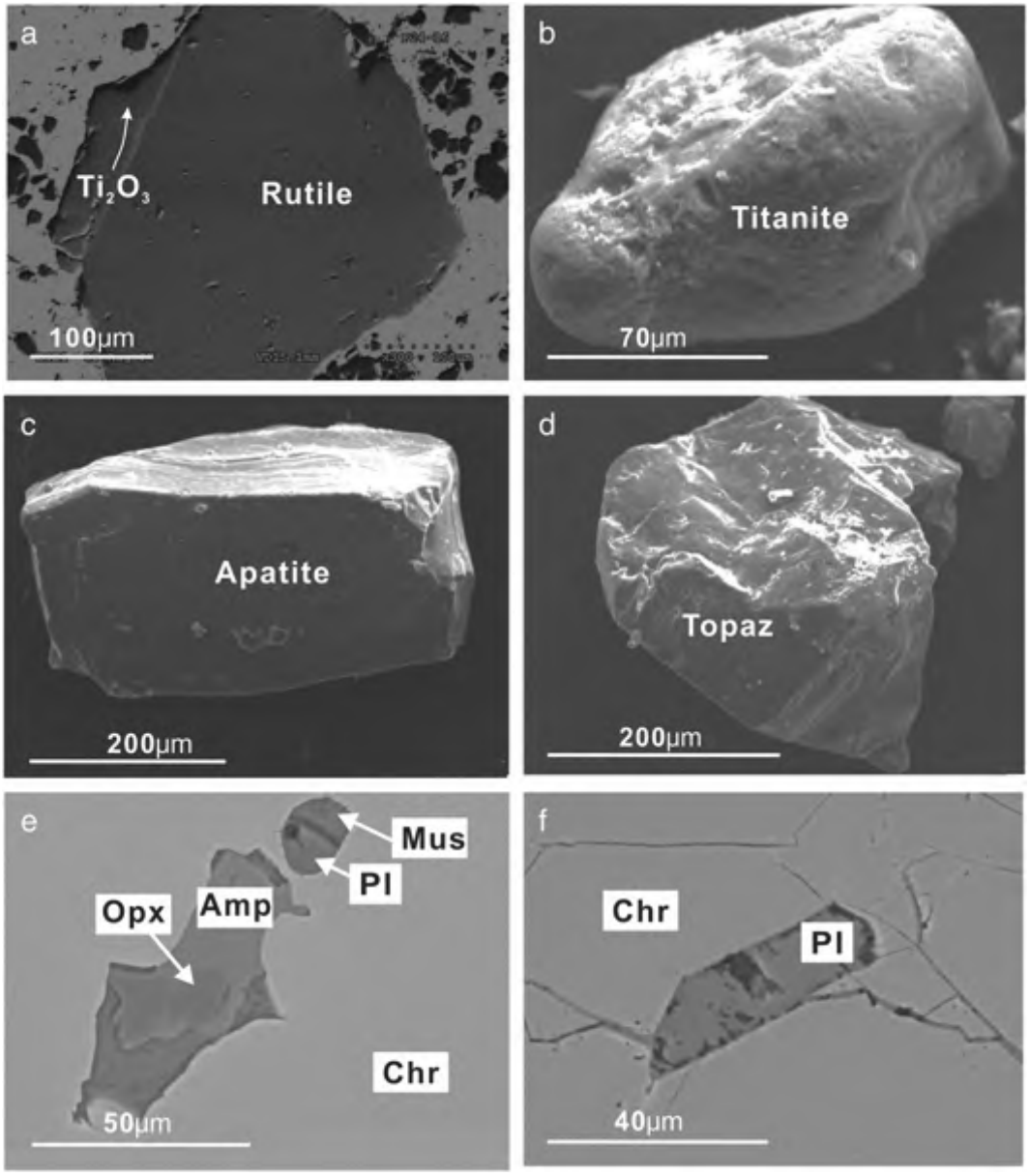

Fig. 11. SEM images of miscellaneous grains recovered from chromitite of the Ray–Iz ophiolite and inclusions in chromite from Luobusa. a) Rutile grain — note small patch of Ti_2O_3 on left side; b) rounded grain of titanite; c) blocky fragment of apatite; d) irregular grain of topaz; e) inclusions of orthopyroxene (Opx), amphibole (Amp); plagioclase (Pl), muscovite (Mus) hosted in chromite (Chr); f) subhedral lath of plagioclase (Pl) hosted in chromite (Chr). Images a–d are from the Ray–Iz ophiolite, e and f are from Luobusa.

well-rounded grains from 50 to 300 μm in diameter (Figs. 12, 13). Very few euhedral grains (e.g., Fig. 13d) are present. Many of the grains contain small inclusions (e.g., Figs. 12e, 13d, g) and microprobe analysis revealed that the inclusions comprise a crustal suite of quartz, muscovite, plagioclase, K-feldspar, ilmenite, rutile and apatite. Cathodoluminescence (CL) and back-scatter electron (BSE) images of polished grains reveal a great variety and complexity of internal structures (Fig. 13). Regular concentric zoning conforming to the grain shape (Fig. 13d) is extremely rare. Typical CL images show irregular, patchy patterns, overgrowths and partial resorption of the grains (e.g. Fig. 13a, c, e, g, h).

Some zircons previously reported from the Ray–Iz chromitites (Lönngren and Kojonen, 2005) are very similar in morphology to those from Luobusa (Fig. 14a) but grains reported by Savelieva et al. (2007) are mostly euhedral to subhedral. Zircon grains that we recovered from Ray–Iz are subrounded to blocky, and typically show evidence of partial melting or resorption (Fig. 14b, c).

6. Zircon compositions

In-situ ICP-MS analyses of zircon from the Luobusa, Dongqiao and Oman ophiolites reveal very uniform major element compositions and generally similar trace element compositions (Appendix II). We did not analyze zircons from Ray–Iz because of their obvious modification (Fig. 14b, c).

Chondrite-normalized, rare earth element (REE) patterns are similar for all grains from the Luobusa, Dongqiao and Oman ophiolites, although the total REE vary considerably, ranging from 98 to 2233 ppm in Luobusa, 268–1930 ppm in Oman and 201 to 1142 ppm in Dongqiao (Appendix II). These relatively high values are typical of zircon formed in silicic rocks. All of the patterns show significant enrichment in HREE with $(La/Sm)_N$ ranging from <0.001 to 118 (Fig. 15). All grains also exhibit moderately negative Eu anomalies and strongly positive Ce anomalies. Contents of Th and U as determined by LA-ICPMS are quite variable (Appendix II), ranging from 2 to 378 ppm Th and 10–1964 ppm U, values generally

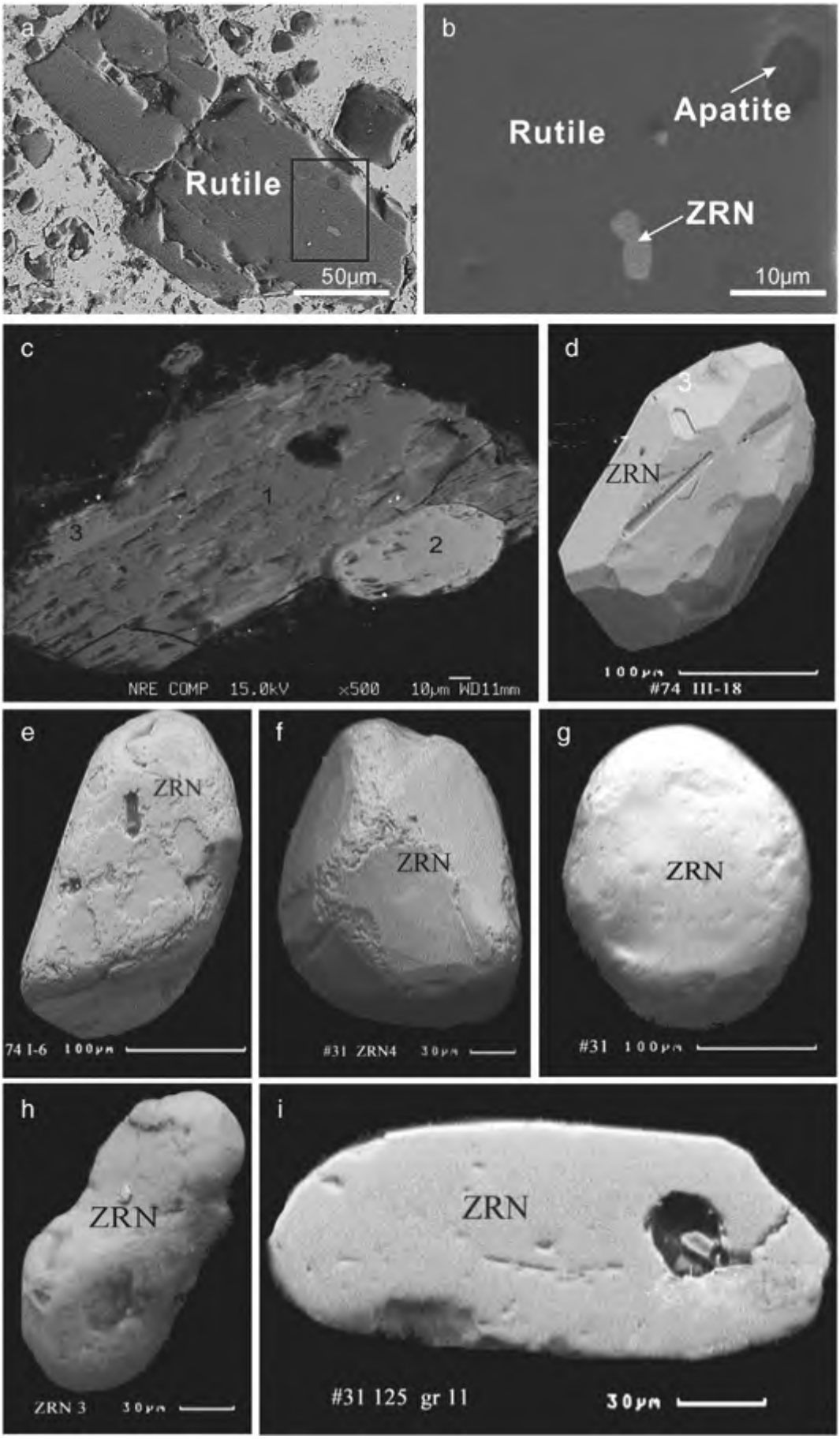
a
Rutile
50μm
b
Rutile
Apatite
ZRN
10μm
c
1
2
3
NRE COMP 15.0kV ×500 10μm WD11mm
d
3
ZRN
100μm
#74 III-18
e
ZRN
74 I-6 100μm
f
ZRN
#31 ZRN4 30μm
g
ZRN
#31 100μm
h
ZRN
ZRN 3 30μm
i
ZRN
#31 125 gr 11
30μm

consistent with a continental provenance. On plots of U vs Yb, U/Yb vs Y and U/Yb vs Hf, all of our analyzed grains plot in the field of continental crust and many lie in the field of continental granitoids as determined by Grimes et al. (2007) (Fig. 16). Variations in the U and Th compositions of the zircons do not correlate with locality, age or position within the grains.

7. Zircon U–Pb geochronology

Forty U–Pb age determinations by SIMS (Appendix III) were made on zircon grains from the Luobusa, Dongqiao and Oman ophiolites. Fourteen grains (16 analyses) from Luobusa yielded $^{206}Pb/^{238}U$ and $^{206}Pb/^{207}Pb$ ages from about 549 to 1675 Ma, all much older than the ophiolite (Fig. 17; Appendix III). We found no correlation between age and morphology, internal structure or composition. Yamamoto et al. (2013) obtained similar ages from Luobusa zircons by LA-ICP-MS but they also reported ages as young as 107 Ma, which post-date the ophiolite and are thus of uncertain significance. Nine zircons (15 analyses) from the Oman ophiolite yielded a similar wide range of $^{206}Pb/^{238}U$ and $^{206}Pb/^{207}Pb$ ages between about 84 and 1411 Ma (Fig. 18; Appendix III). Four grains have late Cretaceous ages essentially the same as the host ophiolite (91–99 Ma) and a fifth grain (OM-1; Appendix III) yielded a $^{206}Pb/^{238}U$ age of 84 ± 4 Ma, which is slightly younger than the ophiolite. Because this grain has visible cracks, and an unusually high U content (1964 ppm) compared with all the other zircons, we suspect that the young age is an artifact of Pb loss. Finally, zircons from the Dongqiao ophiolite (5 grains, 10 analyses) yielded the widest range of $^{206}Pb/^{238}U$ and $^{206}Pb/^{207}Pb$ ages, from about 484 to 2695 Ma (Fig. 18; Appendix III).

Savelieva et al. (2007) dated 9 grains of zircon from the Ray–Iz chromitites. Seven subhedral to euhedral prisms yielded an average age of 585 ± 6 Ma, which is close to the assumed age of the ophiolite. These zircons were attributed to percolation of mafic melts through the mantle sequence in response to Vendian rifting. The other grains are angular to rounded and yielded ages of 622 and 2574 Ma. We did not date the zircon we recovered from this ophiolite because of the strong evidence of melting or corrosion (Fig. 14b, c).

Fig. 19 is a relative frequency plot of measured zircon ages from the Luobusa, Dongqiao and Oman ophiolites showing that all but 4 analyzed grains are older than 300 Ma.

8. Discussion and implications

All of the podiform chromitites examined in this study lie in upper mantle sections of ophiolites within a few kilometers stratigraphically of the crust–mantle boundary. Ophiolites are widely accepted as fragments of oceanic lithosphere but there is considerable disagreement regarding their environment of formation and their mechanism of emplacement on continental margins and in island arcs. Early studies of ophiolites, particularly those focused on structural characteristics, mostly identified them as fragments of typical oceanic lithosphere formed at mid-ocean spreading ridges (e.g. Gass, 1968; Moores and Vine, 1971; Girardeau et al., 1985; Nicolas and Boudier, 2003) However, the geochemistry of ophiolitic basalts and gabbros provides clear evidence for formation and/or modification of ophiolites in suprasubduction zone environments (Pearce, 1975, 2003; Robinson et al., 2003; Rollinson and Adetunji, 2013; Dilek and Furnes, 2014). The presence of boninitic magmas in many ophiolites points to formation in forearc environments during the early stages of subduction imitation (Stern and Bloomer, 1992; Pearce and Robinson, 2010; Stern et al., 2012).

The current understanding for the origin of podiform chromitites is that they form by precipitation of chromite from arc tholeiitic or boninitic magmas undergoing melt–rock reaction with peridotites in SSZ mantle wedges (Zhou et al, 1996; Rollinson, 2005; Rollinson and Adetunji, 2013; González-Jiménez et al., 2013). Formation in suprasubduction zones is also suggested by the common presence of hydrous mineral inclusions in most chromitites. However, chromitites in all four of the ophiolites investigated in this study contain unusual collections of minerals that are difficult to reconcile with this model for ophiolite formation. Chromitites in three of the ophiolites contain UHP minerals and all four contain highly reduced phases, such as native elements, metallic alloys and moissanite, as well as many crustal minerals as described above.

The chromitites preserve textures and compositions typical for such rocks in ophiolites worldwide, and therefore, the discovery of a very similar suite of crustal minerals in four separate bodies of different age and location suggests that such minerals are common in ophiolites. We also emphasize that most of the minerals found in the chromitites have also been recovered from the host harzburgites. Although further work is needed to confirm our interpretation, we suggest that UHP, highly reduced and crustal minerals may be widespread in the oceanic mantle, albeit in small quantities. The diamonds indicate derivation from depths >150 km, whereas coesite pseudomorphs after stishovite (Yang et al., 2007) imply depths of formation >300 km. Coesite and clinopyroxene exsolution lamellae in some chromite grains from Luobusa suggest crystallization of a precursor with a Ca-ferrite structure at depths >380 km Yamamoto et al. (2009). Oxygen fugacity appears to be the most important factor controlling crystallization of moissanite (Trumbull et al., 2009).

A characteristic feature of podiform chromitites is that they are not uniformly distributed in ophiolite belts but rather occur in clusters within individual massifs. For example, the only significant chromitites in the nearly 2000-km-long Yarlung Zangbo suture zone, which contains numerous ophiolitic blocks, occur in the Luobusa massif. And even these comprise a group of relatively small, isolated bodies. By its very existence, any ore deposit is a geochemical anomaly, owing its formation to the concentration of specific elements far beyond their background levels in Earth's crust and mantle. Thus, the formation of podiform chromitites, and the ophiolites in which they occur, must record non-uniform processes.

Seismic tomography suggests that lithospheric slabs can be subducted into the mantle transition zone or even deeper, but it is difficult to see how many of the crustal minerals described here could be preserved under conditions existing at such depths. Some grains, for example, the coesite–kyanite assemblage shown in Fig. 6a, b appears to have grown by reaction between silicic material and an FeTi alloy suggesting crystallization at a depth of >300 km if the coesite grains are pseudomorphs after stishovite (Yang et al., 2007). Likewise, some of the corundum grains contain inclusions of TiSi alloys (Fig. 7d) indicating deep crystallization or recrystallization. However, most of the crustal minerals (zircon, garnet, rutile, quartz, feldspar, titanite, apatite, andalusite and some of the kyanite grains) show little or no evidence of reaction with their host rocks. Many of these, such as quartz, titanite, garnet and particularly zircon occur as abraded or well-rounded grains. Rounding can be caused by mechanical abrasion during sedimentary transport or by chemical processes (resorption or overgrowths) in metamorphic or igneous environments. In the case of zircon, one of the most stable and chemically resistant minerals in crustal rocks (Williams, 2001), rounding of grains may be best attributed to sedimentary transport (Moecher and Samson, 2006). Rounded grains of zircon have been described from many high-grade metamorphic rocks, commonly as cores in euhedral to subhedral grains, and it appears that rounding can also be developed by metamorphic overgrowths (e.g. Corfu et al., 2003). However, the zircon grains described here have low-temperature and low-pressure

Fig. 12. Zircon and rutile grains from the Ray–Iz and Luobusa ophiolites. a) SEM image of tabular rutile grain from the Ray–Iz ophiolite with inclusions of zircon and apatite within the black square: b) enlarged view of the square in (a) showing inclusions of zircon and apatite; c) SEM image of a tabular grain of rutile from the Luobusa ophiolite with inclusion of rounded zircon (KCr-11-7). Irregular light-colored material (3) is Fe,Mn)TiO_3; d–i) SEM images of rounded zircon grains from chromitites of the Luobusa ophiolite.

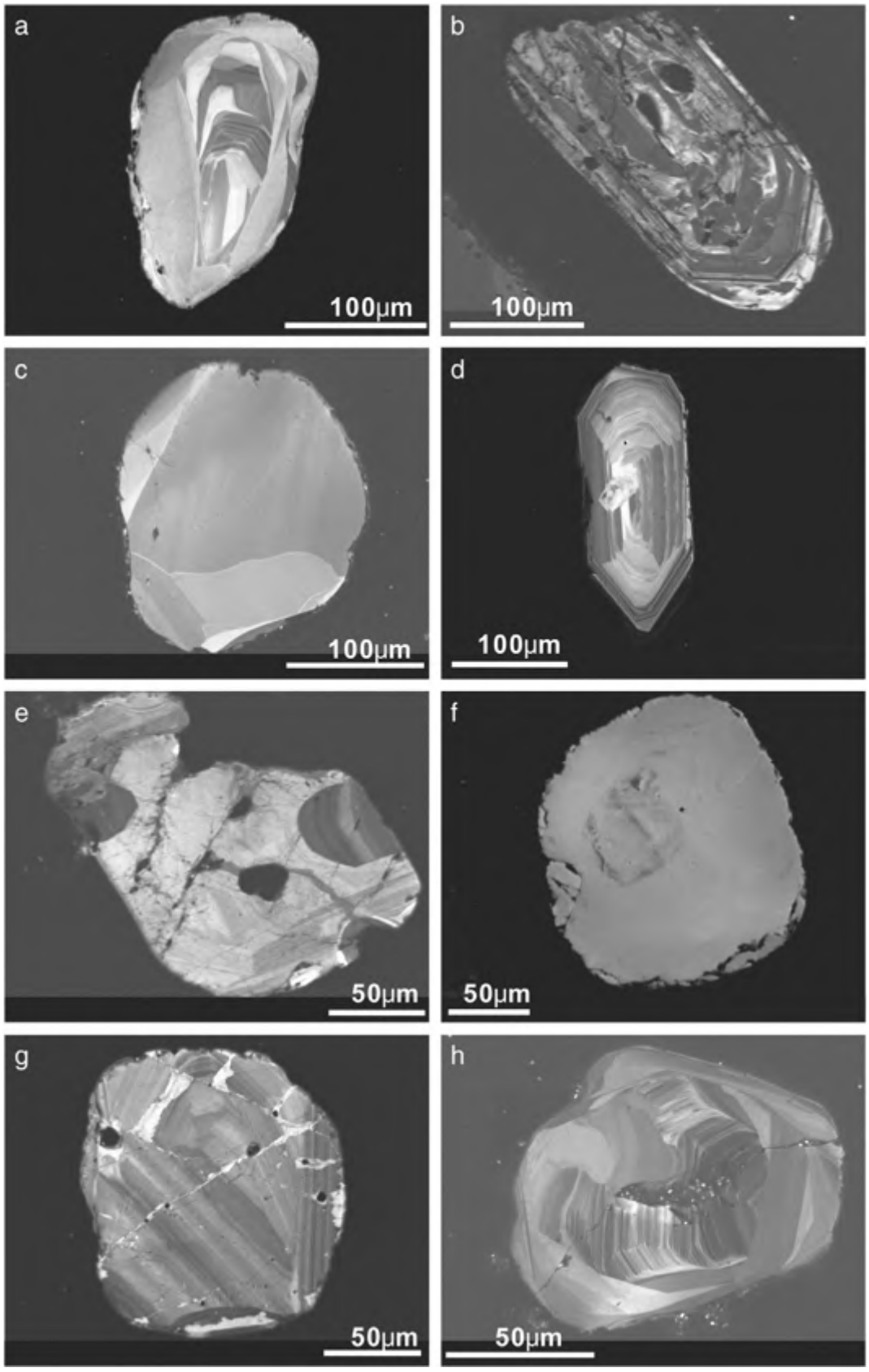

Fig. 13. SEM images of zircon grains from the Luobusa ophiolite showing complex internal textures. a) Partially rounded zircon grain with distinct, zoned core surrounded by several overgrowths; b) fragment of slightly abraded, tabular zircon grain showing an indistinct core rimmed by well-zoned younger zircon; c) rounded zircon grain about 150 μm in diameter with a featureless light gray core partially surrounded by brighter rims: d) euhedral zircon grain about 150 μm long with well-developed concentric zoning. The grain has no obvious overgrowths but contains an inclusion of quartz; e) highly irregular zircon grain about 100 μm long, showing multiple stages of resorption and regrowth; f) rounded zircon grain about 150 μm across with distinct core surrounded by a featureless rim; g) rounded zircon grain about 100 μm across that appears to have a weakly zoned core partly surrounded by a well-zoned rim. The small, black grains are magnetite; h) round zircon grain about 150 μm across with a complexly zoned core surrounded by featureless zircon.

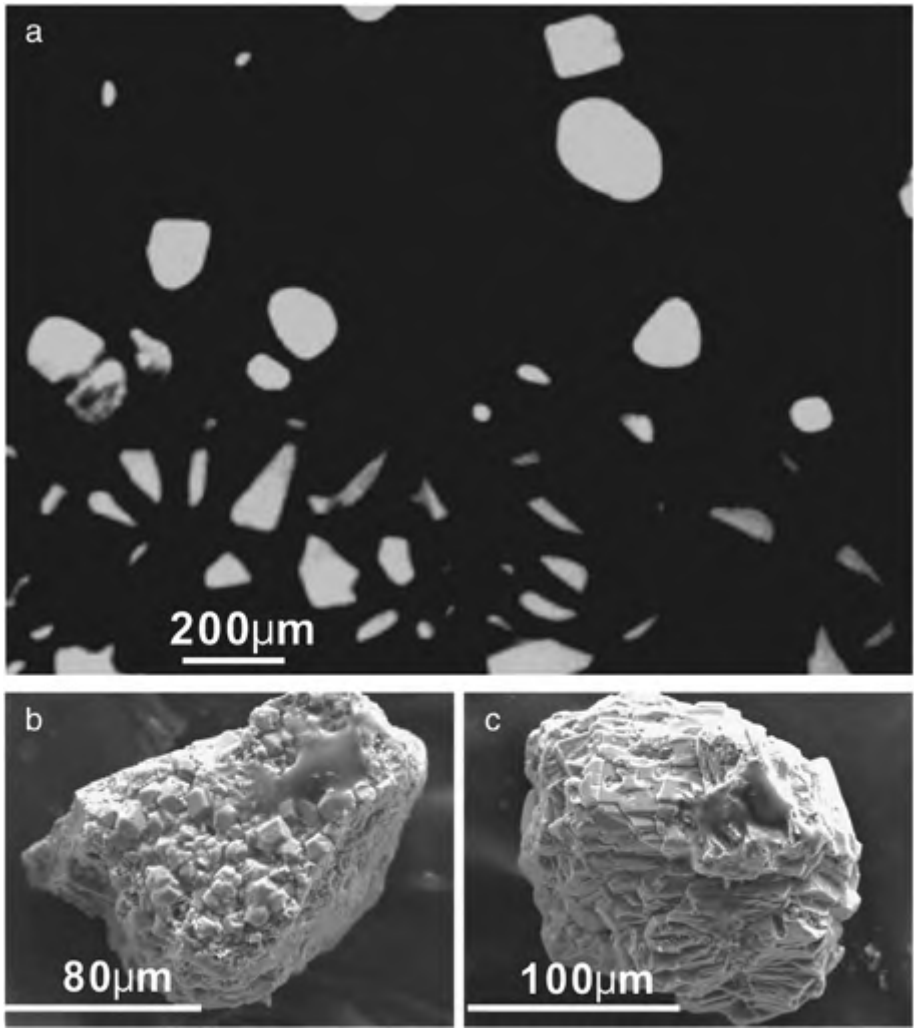

Fig. 14. Zircons recovered from the Ray–Iz ophiolite. a) Round and angular grains of zircon separated from chromitite by dissolution (Lönngren and Kojonen, 2005). b, c) Irregular zircon grains separated mechanically from Ray–Iz chromitite (this study). Note the highly corroded and resorbed nature of these grains, which we attribute to reaction with melts or hydrothermal solutions.

mineral inclusions and commonly show a strong discordance between their external shape and internal zoning (Fig. 13). Thus, we interpret these to be mechanically abraded grains derived from subducted sediments or (meta)sedimentary rocks of crustal origin. The inclusion suite found in the zircons (quartz, muscovite, biotite, feldspar, ilmenite, rutile, apatite), the Paleozoic to Precambrian ages of most grains, and

Table 2
Microprobe analyses of alumino-silicates and corundum from the Luobusa and Ray–Iz ophiolites.
Sources: 1) Yang et al., 2007; 3) Hu, 1999; 4) Xu et al., 2009; 2, 5, 6, 7, 8) unpublished data.

	1	2	3	4	5	6	7	8
Mineral	Kyan	Kyan	Sill	And	Cor	Cor	Cor	Cor
Ophiolite	L	R	L	L	L	L	R	R
Sample		R23-9	B5	Ky-7-2-5	IV	LR4070	lk3.11	P35-8
# Analyses	1	1	10	1	4	1	1	1
SiO_2	38.17	41.4	37.22	37.58	0.09	b.d.	0.01	b.d.
TiO_2	1.98	b.d.	0.05	0.08	0.99	0.40	2.07	b.d.
Al_2O_3	61.49	58.55	62.51	62.07	99.81	98.46	97.71	100.00
Cr2O3	b.d.	b.d.	b.d.	b.d.	b.d.	b.d.	b.d.	b.d.
FeO	b.d.	b.d.	0.21	0.26	0.02	0.03	b.d.	b.d.
MnO	b.d.	b.d.	0.05	0.02	b.d.	0.01	b.d.	b.d.
MgO	b.d.	b.d.	0.10	0.05	0.20	0.01	0.10	b.d.
CaO	b.d.	b.d.	0.04	b.d.	0.01	b.d.	b.d.	b.d.
Na_2O	b.d.	b.d.	0.02	0.01	b.d.	b.d.	0.03	b.d.
K_2O	b.d.	b.d.	0.06	b.d.	b.d.	b.d.	b.d.	b.d.
P_2O_5	b.d.	b.d.	0.05	b.d.	b.d.	b.d.	b.d.	b.d.
BaO	b.d.	b.d.	b.d.	b.d.	b.d.	b.d.	b.d.	b.d.
Total	101.64	99.95	100.31	100.07	101.13	98.91	99.92	100.00

Analyses 2 and 8 by EDS. L = Luobusa, R = Ray–Iz. b.d. = below detection, Kyan — kyanite; Sill — sillimanite; And — andalusite; Cor — corundum.

Table 3
Microprobe analyses of quartz and moissanite from the Loubusa and Ray–Iz ophiolites.
Source: Unpublished data.

Mineral	Quartz			Moissanite		
Sample	LR-2	LK8	R29-39	LR4070-6	LR4070-2	LR-3
Ophiolite	L	L	R	L	L	L
SiO_2	97.87	98.52	100.00	70.61	76.69	77.16
TiO_2	b.d	0.01	b.d	0.01	0.01	0.03
Al_2O_3	b.d	0.27	b.d	b.d	b.d	b.d
FeO	0.93	0.05	b.d	b.d	b.d	0.01
MnO	0.20	0.03	b.d	b.d	b.d	b.d
MgO	0.00	0.04	b.d	b.d	b.d	b.d
CaO	0.00	0.17	b.d	b.d	b.d	b.d
Na_2O	0.01	0.05	b.d	b.d	b.d	b.d
K_2O	b.d	0.03	b.d	b.d	b.d	b.d
P_2O_5	0.01	0.00	b.d	b.d	b.d	b.d
BaO	b.d	0.00	b.d	b.d	b.d	b.d
C	b.d	0.00	b.d	29.25	22.47	21.96
	99.02	99.17	100.00	99.87	99.17	99.16

L — Luobusa, R = Ray–Iz b.d = below detection.

the polyphase history implied by their internal textures suggest derivation from heterogeneous, felsic, crystalline rocks. The trace element compositions of these grains, particularly their elevated U and Th contents, are consistent with a felsic crustal source (Grimes et al., 2007). Therefore, all available data suggest that the rounded zircons are detrital grains from crustal sources and we infer that most of the other crustal minerals were likely derived from similar sources. So, the fundamental question is how such minerals were introduced into the podiform chromitites and how were they preserved in such a hostile environment?

Clearly, the ages of the recovered zircons do not necessarily correspond to the time at which they were introduced into the mantle. Old grains could have been introduced or recycled into the mantle at any time after their formation. The range of UHP, highly reduced and crustal minerals found in chromitites suggests a complex origin for these deposits and the ophiolites in which they occur. It seems likely that several processes may be acting in concert but that different combinations of processes may have operated in different ophiolites.

Any model for the formation of ophiolites and podiform chromitites must explain the mixture of very different minerals in these bodies, the preservation of UHP, highly reduced and crustal minerals far outside their normal stability fields, and the evidence for both deep and shallow crystallization of chromite.

On the basis of tomographic evidence and ages of confirmed ophiolites, we assume that for at least the last 2500 m.y. slabs of oceanic crust and lithosphere have been carried into the mantle transition zone and probably deeper (Condie and Kröner, 2008). The occurrence of highly reduced minerals in the upper mantle argues for addition of this material from a deeper source, perhaps by C-rich fluids, relics of which are preserved in the chromitites as carbon spheres, currently hosting diamonds and highly reduced minerals. Thus, subducted crustal material and highly reduced fluids can be mixed in, or near, the mantle transition zone. Most crustal material would not be stable under such conditions and would presumably react with the highly reduced phases, as apparently happened with formation of the coesite–kyanite assemblage described above. The stability of zircon under such conditions is uncertain, but it seems to us unlikely that zircon grains containing inclusions of low-pressure crustal minerals would remain unmodified over long periods of time.

Magnesiochromite is stable to depths equivalent to about 14 GPa, at which point it breaks down to a precursor with a Ca-ferrite structure (Yamamoto et al., 2009; Jin et al., 2014). Thus, chromite grains can crystallize readily in the upper mantle as indicated by their common presence in oceanic peridotites. Chromite grains crystallizing under these conditions can encapsulate small pockets of C-rich fluid that carry UHP minerals (e.g., diamonds — Robinson et al., 2013), highly reduced phases (moissanite — Fig. 9d) and crustal minerals (corundum — Fig. 7e, f). Such encapsulated minerals would be at least partially protected from melts produced in the rising asthenosphere beneath a spreading ridge. Some chromite grains might adhere to one another to form small chromitite pods (e.g., Arai and Matsukage, 1998; Abe, 2011) but there is, as yet, no evidence that major podiform chromitites form in the deep mantle; in fact, the available evidence points unquestionably to chromitite crystallization from hydrous, high Si-high Mg magmas in suprasubduction zones (Rollinson and Adetunji, 2013).

So, how are UHP, highly reduced and crustal minerals introduced into suprasubduction zone mantle wedges containing podiform chromitites that eventually become ophiolites? If UHP and highly reduced minerals are widespread in the modern oceanic mantle, they could be trapped in SSZ mantle wedges by formation of intra-oceanic subduction zones (Fig. 20a). The descending lithospheric slab carries not only crustal basalts and gabbros but sedimentary rocks, some of which were derived from continental sources. Continent-derived sediment on the oceanic plate could be mixed with the other minerals and be incorporated into the mantle peridotites and chromitites that eventually become emplaced as ophiolites. This model basically

Table 4
Microprobe analyses of garnet from Semail, Luobusa and Ray–Iz ophiolites.
Source: B, IV, VI samples are from Hu (1999); others are unpublished data.

Sample	GII	GIV	IV	LR-2.7	B3	VI	LR2	IR11	R32	Va-20	LR22
Ophiolite	S	S	L	L	L	L	LR2	R	R	R	L
Mineral	Almandine				Fe–Mn Garnet					Uvarovite	
SiO_2	36.71	35.53	36.73	38.56	37.20	36.89	36.46	35.01	39.03	35.11	36.82
TiO_2	b.d.	b.d.	0.01	0.05	0.04	0.02	0.04	b.d.	n.d.	0.68	n.d.
Al_2O_3	21.27	20.50	20.85	21.96	21.03	20.58	21.45	20.76	19.71	0.55	n.d.
Cr_2O_3	b.d.	b.d.	0.01	0.03	0.02	0.01	0.09	0.00	0.00	27.84	28.40
FeO	39.74	40.75	38.98	21.28	29.52	21.50	30.52	15.43	19.72	1.15	1.54
MnO	0.29	0.32	0.40	0.31	5.80	15.70	7.13	28.22	21.54	0.00	n.d.
MgO	2.47	1.92	2.35	5.95	3.22	3.33	1.48	n.d.	n.d.	0.12	n.d.
CaO	1.02	0.86	1.03	11.67	3.80	1.41	3.71	0.49	0.00	33.80	33.24
Total	101.58	99.85	100.36	99.81	100.63	99.41	100.88	99.91	100.00	99.25	100.00
Almandine	86.3	88.6	86.5	43.9	63.0	46.5	66.5	30.2	47.5	0.0	3.3
Pyrope	10.0	8.0	9.5	23.0	12.9	13.4	6.1	n.d.	n.d.	0.5	0.0
Grossular	2.8	2.3	2.9	31.3	10.4	3.9	10.3	1.4	0.0	2.6	0.0
Spessartine	0.7	0.8	0.9	0.7	13.2	36.0	16.6	68.3	52.5	0.0	0.0
Uvarovite	0.0	0.0	0.0	0.0	0.0	0.0	0.0	0.0	0.0	89.7	96.4
Andradite	0.2	0.2	0.1	1.0	0.5	0.1	0.5	0.1	0.0	7.1	0.4

S — Semail; R — Ray–Iz; L —Luobusa. b.d. = below detection. Analysis LR22 by EDS.

Table 5
Microprobe analyses of miscellaneous minerals from the chromitites of the Luobusa and Ray–Iz ophiolites.
Source: 3, IV, B3 samples from Hu (1999). Other samples are unpublished data.

Mineral	Rutile					Titanite				Apatite				Hornbl	Biotite
Ophiolite	L	L	L	L	L	L	L	L	R	L	L	L	R	L	L
Sample	3	KCr	LR3	p15-5	KCr-11	IV-48	LR-3.7	LR4.22	R26-7-2	IV-32	LK1-3b	LR3.12	R21-5	3	B3
SiO_2	0.02	0.02	0.02	b.d.	0.43	29.90	30.72	30.72	31.32	b.d.	b.d.	b.d.	b.d.	42.48	37.65
TiO_2	99.50	98.26	99.53	100.00	52.56	34.31	36.72	36.72	38.55	b.d.	0.02	0.01	b.d.	2.90	1.27
Al_2O_3	b.d.	0.03	0.02	b.d.	0.05	1.46	1.34	1.34	1.71	b.d.	0.03	0.01	b.d.	10.46	19.68
FeO	0.50	0.41	0.47	b.d.	31.41	1.57	1.54	1.54	b.d.	0.04	0.12	0.09	b.d.	8.42	15.71
MnO	b.d.	0.02	0.00	b.d.	15.26	0.18	0.02	0.34	b.d.	0.08	0.06	0.23	b.d.	0.01	0.12
MgO	b.d.	b.d.	0.02	b.d.	0.03	0.01	b.d.	b.d.	b.d.	0.04	0.04	b.d.	b.d.	15.84	11.35
CaO	b.d.	0.03	0.01	b.d.	0.07	27.84	27.98	27.98	28.42	56.44	56.82	55.65	49.67	11.68	0.01
Na_2O	b.d.	b.d.	0.02	b.d.	b.d.	0.03	b.d.	b.d.	b.d.	0.13	0.06	0.06	b.d.	2.91	0.45
K_2O	b.d.	b.d.	b.d.	b.d.	b.d.	b.d.	b.d.	b.d.	b.d.	0.01	b.d.	0.01	b.d.	1.35	7.77
P_2O_5	b.d.	b.d.	0.03	b.d.	b.d.	0.07	b.d.	0.29	b.d.	41.89	43.11	43.19	50.33	0.07	0.03
Total	100.02	98.77	100.12	100.00	99.81	95.35	98.32	98.93	100.00	98.63	100.26	99.25	100.00	96.11	94.04

R — Ray–Iz, L — Luobusa. b.d. = below detection. Analyses P15-5 and R21-5 by EDS.

follows the work of Stern and Bloomer (1992) and Stern et al. (2012) that calls for ophiolite formation in fore-arc regions (Fig. 20a), a model supported by the common presence of high-Mg boninitic lavas in such environments.

Podiform chromitites are currently thought to form from arc tholeiite and boninitic magmas generated by hydrous melting of peridotites in SSZ wedges and there is clear evidence that high-Cr chromite can be formed by reaction between hydrous melts and harzburgites in SSZ mantle wedges (Zhou et al., 1996). However, this model alone does not account for the presence of UHP and highly reduced minerals in the chromitites, nor can it account for the large volumes of mafic, Cr-bearing magma required to produce even a small chromitite body. Given Earth's mantle is estimated to have somewhere between 0.3 wt.% and 0.7 wt.% Cr_2O_3 and that even the most mafic magmas generally have less than 20 ppm Cr, it is not possible to produce a podiform chromitite by simple crystallization of a single, static pod of magma (Zhou et al., 2014). Thus, we conclude that podiform chromitites must be formed either by precipitation from large volumes of magma migrating through upper mantle peridotites, and/or by aggregation of magnesiochromite grains that are widespread in the upper oceanic mantle.

Experimental study suggests that chromite can crystallize at any depth in Earth above 400 km. We suggest that as chromite crystallizes above the Transition Zone it encapsulates UHP minerals such as diamonds and stishovite/coesite and highly reduced phases such as moissanite, native elements and metallic alloys that are stable at these depths. The circular patches of amorphous carbon, in which most of the in-situ grains occur, suggest the presence of a carbon-rich fluid in which these phases probably already existed. Convective rise brings these peridotites to shallow levels and distributes them widely in the upper oceanic mantle. The UHP and highly reduced minerals are preserved at shallow levels because they are encapsulated in chromite grains that protect them from the ambient environment.

Sinking and rollback of lithospheric slabs during initiation of intra-oceanic subduction zones allows asthenospheric peridotites to rise into the forearc region (Fig. 20a), where they may undergo partial melting. Partial melting of the suprasubduction zone peridotites in the mantle wedge produces hydrous arc tholeiite and boninitic magmas that rise through the wedge and react with the peridotites. Chromite grains in the peridotites are mobilized by SSZ melts and fluids, are modified in composition, reprecipitated and redistributed to form podiform bodies containing diamonds, highly reduced phases and crustal minerals.

The crustal minerals are believed to have been introduced into the upper mantle during subduction initiation. Some of the crustal material on the downgoing slab is scraped off and added to the mantle wedge where it is also incorporated into rapidly crystallizing chromite grains. Chromite crystallization in this environment may be triggered by changes in magma composition produced by melt/rock reaction and/or assimilation of some of the crustal material (Zhou et al. this volume).

Earlier subduction of lithospheric slabs may have carried crustal material to much greater depths, perhaps to the Transition Zone where it reacted with some of the deep mantle phases (e.g., coesite and kyanite rimming an FeNi alloy) (Fig. 6). The UHP, highly reduced and crustal minerals are preserved in the chromitites because they are isolated from their surroundings. It is not yet clear how such minerals are preserved in the associated mantle peridotites but, wherever in situ grains

Table 6
Microprobe analyses of plagioclase and K-feldspar from the Luobusa ophiollite.
Source: B samples from Hu (1999). Other samples are unpublished data.

Mineral	Plagioclase					K-Feldspar				
Sample	B5	B6	B7	B9	4070-4	B2	4070-2	4070-8	LR-6	lk6-25
SiO_2	60.77	61.80	60.59	57.51	61.68	64.32	66.80	65.90	64.49	70.43
TiO_2	0.02	b.d.	b.d.	0.09	b.d.	0.04	b.d.	0.01	0.04	0.04
Al_2O_3	24.22	24.59	25.57	27.78	24.37	18.46	17.83	18.74	18.20	18.11
FeO	0.04	0.01	0.01	0.17	0.07	0.01	0.12	b.d.	0.05	0.01
MnO	0.03	0.04	b.d.	b.d.	b.d.	0.01	0.03	b.d.	b.d.	0.00
MgO	0.04	0.07	0.04	0.02	b.d.	0.04	b.d.	b.d.	b.d.	0.00
CaO	6.24	6.25	7.50	10.00	5.33	0.05	b.d.	0.01	b.d.	0.00
Na_2O	7.67	7.57	7.17	5.45	7.39	1.51	0.48	0.02	1.07	0.18
K_2O	0.20	0.05	0.02	0.21	0.28	13.49	15.62	15.45	15.60	11.65
Total	99.28	100.46	100.90	101.23	99.12	98.89	100.88	100.13	99.45	100.42
An	30.7	31.2	36.6	49.7	28.0	0.3	0.0	0.1	0.0	0.0
Ab	68.2	68.5	63.3	49.0	70.2	14.5	4.5	0.2	9.4	2.3
Or	1.1	0.3	0.1	1.2	1.8	85.2	95.5	99.7	90.6	97.7

All samples are from the Luobusa ophiolite. b.d. = below detection.

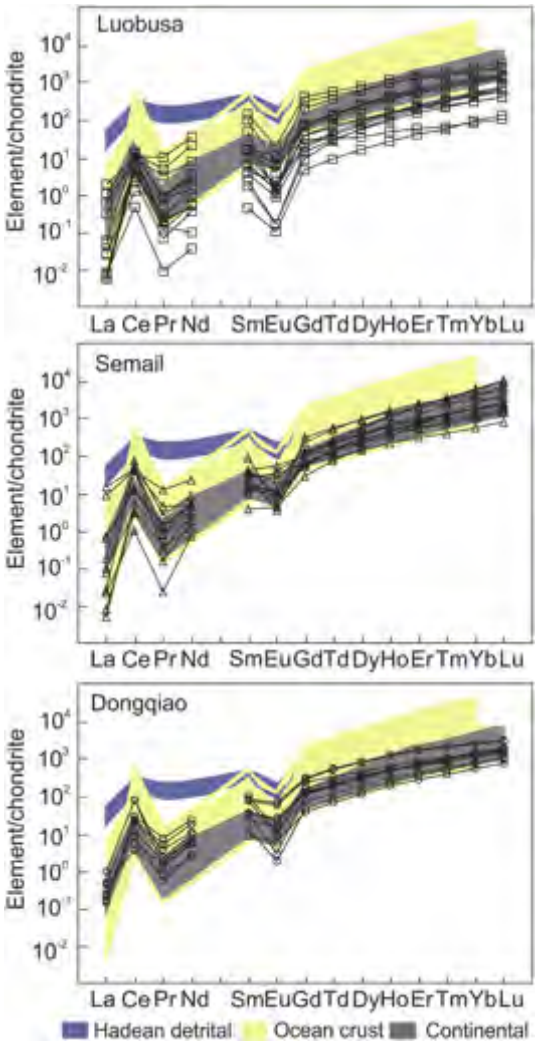

Fig. 15. Chondrite-normalized rare earth patterns for zircon from the Luobusa, Semail and Dongqiao ophiolites. Most grains plot in the field of continental zircon (Grimes et al., 2007), although some, such as those from the Semail ophiolite, have lower total REE.

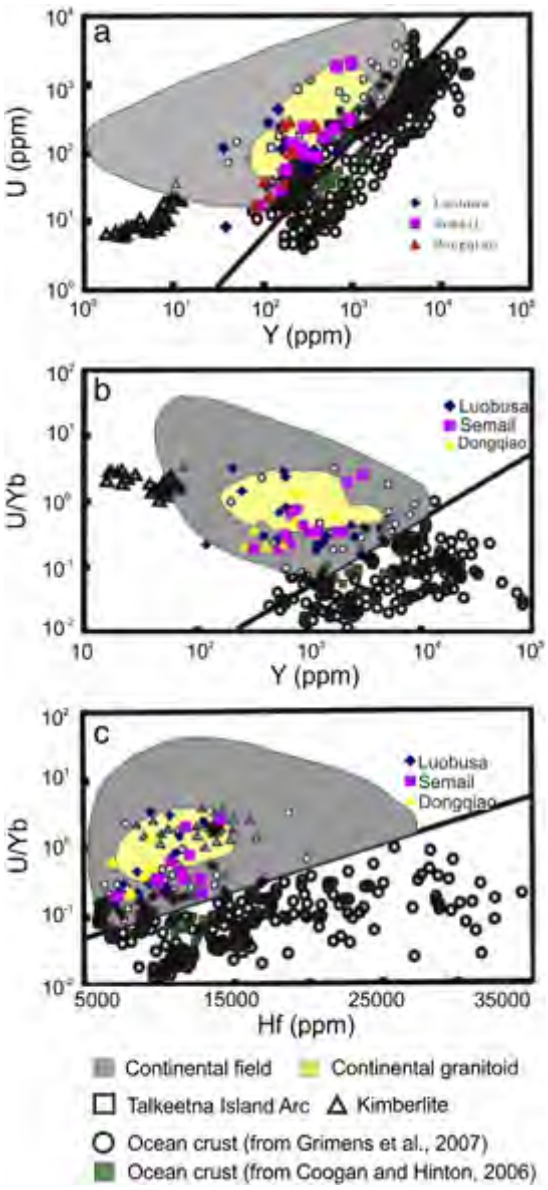

Fig. 16. Trace element plots of zircon from the Luobusa, Semail and Dongqiao ophiolites. a) U vs Yb; b) U/Yb vs Y; c) U/Yb vs Hf. Note that all of the analyzed zircons plot in the continental field and most plot within the continental granitoid field as defined by Grimes et al. (2007).

have been found in the peridotites they are hosted chromite or olivine (e.g., Figs. 7f and 9d).

In our model, ophiolites form chiefly in fore-arc and back-arc environments. Proto-ophiolites formed in fore-arcs commonly contain boninites and high-Cr chromitites. High-Al, refractory chromitites are thought to form from less mafic magmas, such as arc tholeiites, which are more common in arc and back-arc environments. Suprasubduction zone ophiolites can be uplifted and emplaced on land when low-density continental crust is dragged down the subduction zone beneath the mantle wedge.

As pointed out above, podiform chromitites are not uniformly distributed in most ophiolite belts but rather cluster in particular peridotite massifs. We speculate that localization of these deposits may be in response to local slab tear, which allows hot, asthenospheric mantle carrying UHP and highly reduced minerals to rise rapidly into the suprasubduction zone wedge (Fig. 20b). Crustal minerals could have been incorporated into the rising peridotites as they passed through the subducting slab.

Zircons have been described from other mantle-derived rocks (e.g. Pilot et al., 1998, but see Hellebrand et al., 2007; Bortnikov et al., 2008; Bea et al., 2001; Peltonen et al., 2003; Grieco et al., 2001; Katayama et al., 2003; Song et al., 2005; Savelieva et al., 2007; Yamamoto et al., 2013), but most of these have been attributed to mantle metasomatism or UHP metamorphism of ultramafic rocks (garnet peridotites). Only Yamamoto et al. (2013) has proposed crustal contamination of the mantle, but they suggested that the zircons were introduced into the mantle by subduction much earlier than the formation of the Luobusa ophiolite. Certainly, crustal material must have been subducted repeatedly through Earth history during subduction of oceanic lithosphere. However, we believe it is unlikely that most of the crustal minerals described here, probably even the zircons, could have persisted for long periods in the upper mantle. These would more likely react with the highly reduced phases, in a manner similar that which formed the coesite–kyanite intergrowth in Luobusa (Fig. 6a, b). In particular, it seems unlikely that the zircons could preserve their low-pressure, silicate inclusions under deep mantle conditions.

Bea et al. (2001) described ancient zircons in the Kytlym dunite of the Ural Mountains of Russia that have some similarities to the ophiolitic varieties described here. However, the Kytlym dunite is part of a zoned dunite–clinopyroxenite–gabbro massif (Alaskan-type intrusion), rather than belonging to an ophiolite. The zircons in Kytlym are thought to

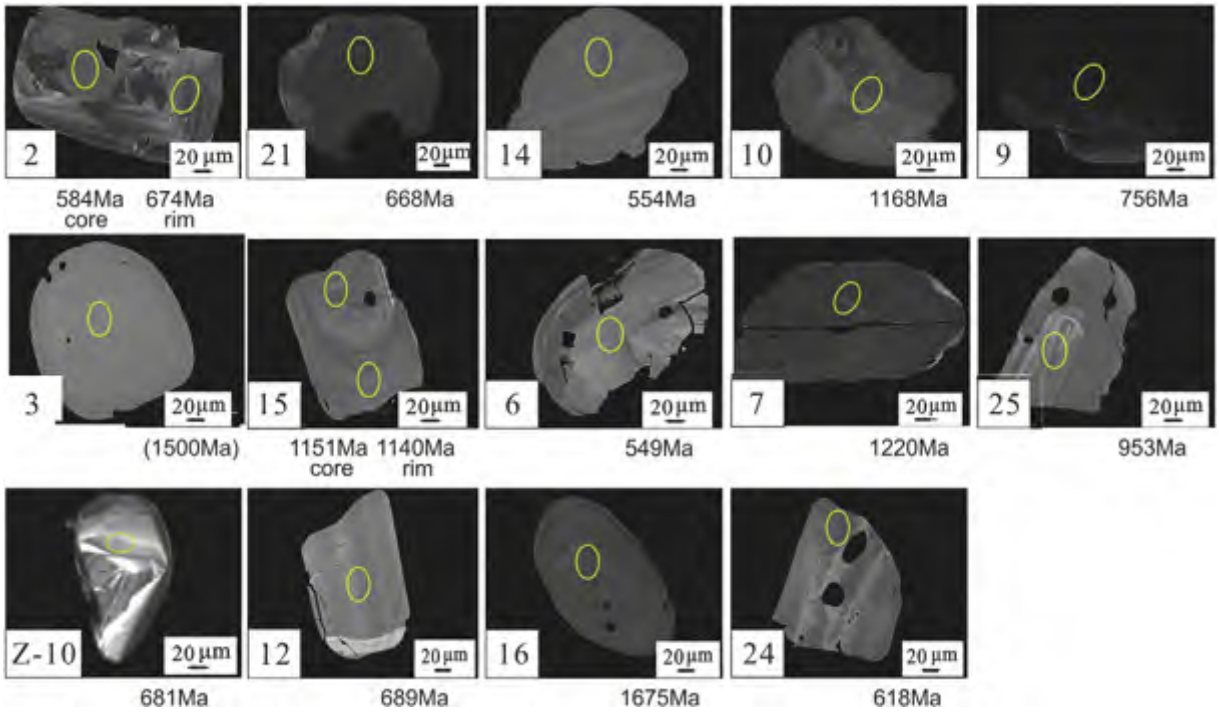

Fig. 17. SIMS geochronology results for zircons from the Luobusa ophiolite. Arabic numbers refers to grains from orebody 31 and are keyed to grains in Appendix III. Grain Z-10 is from orebody 74. The brackets on the age of grain 3 indicate large uncertainty and this grain is not listed in Appendix III. The ellipses mark the locations of the analytical spots.

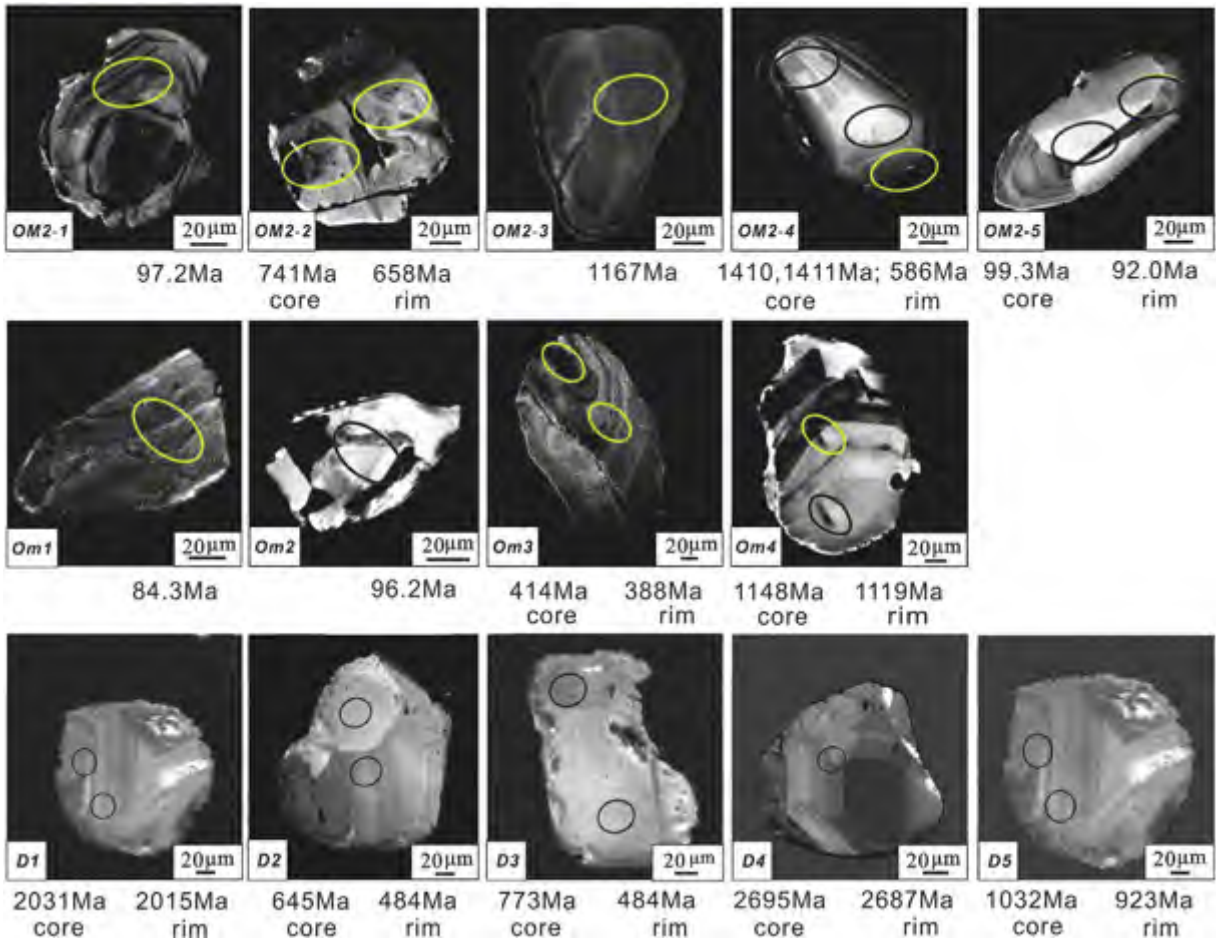

Fig. 18. SIMS geochronology results for zircons from the Semail and Dongqiao ophiolites. OM samples are from the Semail ophiolite and D samples are from the Dongqiao body. Analyzed zircons from the Semail ophiolite range from 84.3 to 1411 Ma and those from Dongqiao from 645 to 2695 Ma.

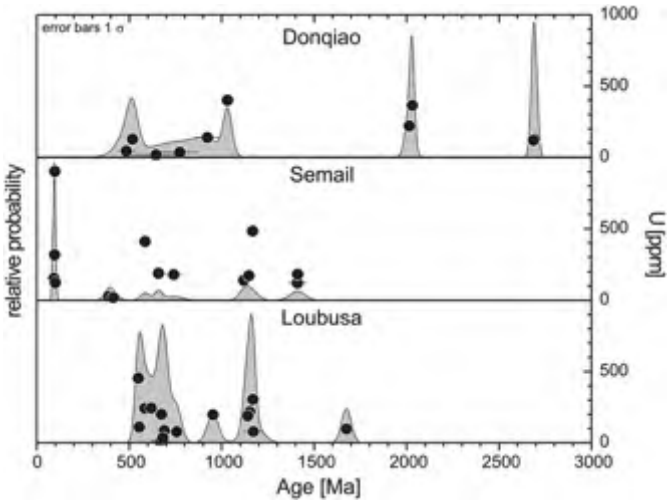

Fig. 19. Diagram showing the relative frequency of zircon ages for the Dongqiao, Semail and Luobusa ophiolites.

reflect a significant sediment-melt component in the magma from which the dunites crystallized.

9. Conclusions

1) Small quantities of continental crustal minerals are widely present in ophiolitic peridotites and chromitites where they are associated with UHP and highly reduced phases. Some of these minerals are thought to have been subducted into the deep mantle where they have reacted with highly reduced phases (coesite–kyanite rimming an Fe–Ti alloy) or been partly or completely recrystallized (corundum with Ti–Si inclusions).
2) Rounded zircon grains with ages much older than the ophiolites in which they occur have inclusions and trace element compositions clearly indicating a crustal origin. They are considered to be derived from metasedimentary rocks introduced into the upper mantle during subduction mostly likely related to formation of the ophiolites in which they now occur.
3) The crustal, UHP and highly reduced minerals in the ophiolites were likely preserved by being encapsulated in chromite grains.
4) Ophiolites form, or are modified, in suprasubduction zone environments, mostly in fore-arc regions. The introduction of UHP, highly reduced and crustal minerals into ophiolites is facilitated by asthenospheric flow into suprasubduction zone wedges during subduction initiation. The localization of podiform chromitites in suture zones may reflect local slab tear, allowing rapid uprise of asthenospheric melts into SSZ mantle wedges.
5) Our results imply that the upper oceanic mantle is more chemically, mineralogically and isotopically heterogeneous than previously thought.

Supplementary data to this article can be found online at http://dx.doi.org/10.1016/j.gr.2014.06.003.

Acknowledgments

We thank Hugh Rollinson (Derby University) for assistance in sampling the Semail ophiolite and for many fruitful discussions on the origin of chromitites. We also thank the Oman Directorate General of Minerals for their support of this project. Professors W.-J. Bai and Q.-S. Fang (deceased), Chinese Academy of Sciences provided invaluable support and encouragement for this project. J. Glodny, H. Kemnitz, M. Gottschalk and D. Rhede, all at the GFZ Potsdam, Germany gave expert assistance with mineral separation and identification. Sandra Kostrowksi assisted greatly in many aspects of the work, particularly in the SEM and microprobe analyses at the GFZ. We benefited from many discussions with I. Veklser (GFZ) regarding mineral stability. We also thank Zhongming Zhang (CAGS) for assistance with preparation of the manuscript. Financial support for this project was provided by the GeoForschungsZentrum, Potsdam and the Chinese Academy of Geological Sciences, Beijing, China.

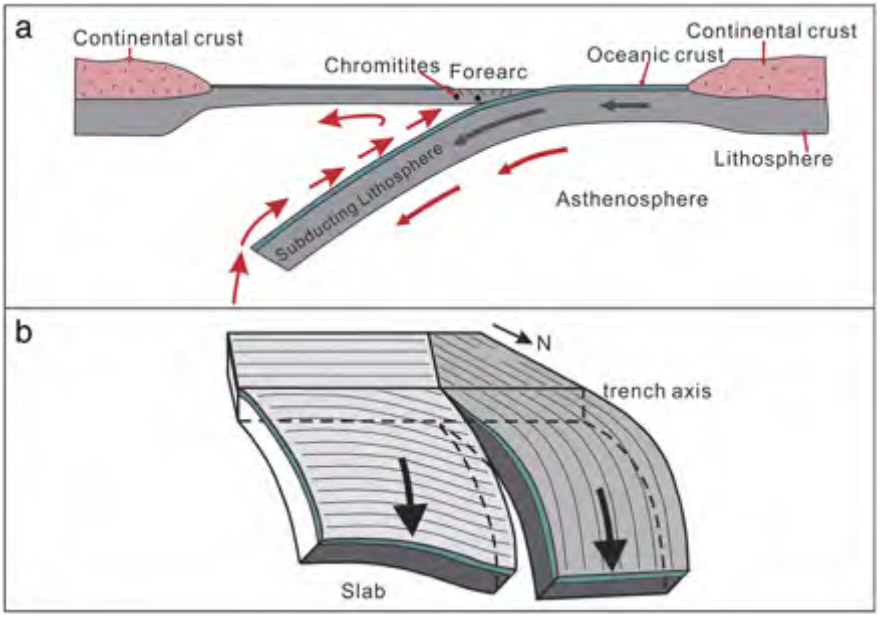

Fig. 20. Proposed model for the formation of ophiolites in suprasubduction zones that provides a mechanism for introduction and preservation of UHP, highly reduced and crustal minerals into SSZ chromitites and peridotites during subduction initiation (cf. Stern and Bloomer, 1992). See text for detailed discussion. a) Subduction initiation in an intraoceanic setting causes rise of asthenospheric mantle and melts into the suprasubduction zone wedge. b) Local tear in subducting slab allows uprise of asthenospheric mantle and melts to shallow levels and allows development of large-scale podiform chromitites with UHP, highly reduced and crustal minerals.

References

Abe, N., 2011. Petrology of podiform chromitite from the ocean floor at the 15°20_NFZ in the MAR, Site 1271, ODP Leg 209. Journal of Mineralogical and Petrological Science 106, 97–102.

Ahmed, A.H., Arai, S., 2002. Unexpectedly high PGE chromitites from the deeper mantle section of the northern Oman ophiolite and its tectonic implications. Contributions to Mineralogy and Petrology 143, 263–278.

Arai, S., Matsukage, K., 1998. Petrology of a chromitite micropod from Hess Deep, equatorial Pacific: a comparison between the abyssal and alpine-type podiform chromitites. Lithos 43, 1–14.

Bai, W.-J., Robinson, P.T., Fang, Q., Hu, X.-F., Zhou, M.-F., 2000. Origin of PGE and base metal alloys in podiform chromitites of the Luobusa ophiolite, southern Tibet. Canadian Mineralogist 38, 585–598.

Bai, W.J., Yang, J.S., Fang, Q.S., Yan, B.G., Zhang, Z.M., 2001. Study on a storehouse of ultrahigh pressure mantle minerals — podiform chromite deposits. Earth Science Frontiers (China University of Geosciences, Beijing) 8, 111–121 (in Chinese with English abstract).

Bai, W.J., Shi, N., Yang, J.S., Fang, Q.S., Ren, Y.F., Rong, H., Li, G.W., Ma, Z.S., 2007. An assemblage of simple oxide minerals from ophiolite podiform chromitites in Tibet and their ultrahigh pressure origin. Acta Geologica Sinica 81, 1538–1549 (in Chinese with English abstract).

Bea, F., Fershtater, G.B., Montero, P., Whitehouse, M., Levin, V.Z., Scarrow, J.H., Austrheim, H., Pushkariev, E.V., 2001. Recycling of continental crust into the mantle as revealed by Kytlym dunite zircons, Ural Mts, Russia. Terra Nova 13, 407–412.

Bortnikov, E.V., Sharkov, E.V., Bogatikov, O.H., Zinger, T.F., Lepekhinar, E.N., Antonov, A.V., Sergeev, S.A., 2008. Finds of young and ancient zircons in gabbroids of the Markov Deep, Mid-Atlantic Ridge, 5°54'-5°02.2'N (Results of SHRIMP-II U-Pb dating): implication for deep geodynamics of modern oceans. Doklady Earth Sciences 421, 854–866.

Condie, K.C., Kröner, A., 2008. When did plate tectonics begin? Evidence from the geologic record. Geological Society of America, Special Paper 440, 281–294.

Corfu, F., Hanchar, J.M., Hoskin, W.O., Kinny, P., 2003. Atlas of zircon textures. Reviews in Mineralogy and Geochemistry 53, 469–500.

Dilek, Y., Furnes, H., 2014. Ophiolites and their origins. Elements 10, 93–100.

Dobrzhinetskaya, L.F., Wirth, R., Yang, J., Hutcheon, I.D., Weber, P.K., Green II, H.W., 2009. High-pressure highly reduced nitrides and oxides from chromitite of a Tibetan ophiolite. Proceedings of the National Academy of Sciences 106, 19233–19238.

Fang, Q.S., Bai, W.J., 1981. The discovery of Alpine-type diamond-bearing ultrabasic intrusions in Tibet. Geological Review 22, 455–457.

Garuti, G., Zaccarini, F., Moloshag, V., Alimov, V., 1999. Platinum-group minerals as indicators of sulfur fugacity in ophiolitic upper mantle: an example from chromitites of the Ray–Iz ultramafic complex, Polar Urals, Russia. Canadian Mineralogist 37, 1099–1115.

Gass, I.G., 1968. Is the Troodos Massif of Cyprus a fragment of Mesozoic ocean floor? Nature 220, 39–42.

Girardeau, J., Mercier, J.C.C., Zao, Y.-G., 1985. Structure of the Xigaze ophiolite, Yarlung Zangbo suture zone, southern Tibet, China: Genetic implications. Tectonics 4, 267–288.

González-Jiménez, J.M., Griffin, W.L., Proenza, J.A., Gervilla, F., O'Reilly, S.Y., Akbulut, M., Pearson, N.J., Arai, S., 2013. Chromitites in ophiolites: how, where, when, why? Part II. The crystallization of chromitites. Lithos. http://dx.doi.org/10.1016/j.lithos.2013.09.008.

Grieco, G., Ferrario, A., Von Quadt, A., Koeppel, V., Mathez, E.A., 2001. The zircon-bearing chromitites of the phlogopite peridotite of Finero (Ivrea Zone, Southern Alps): evidence and geochronology of a metasomatized mantle slab. Journal of Petrology 42, 89–101.

Grimes, C.B., John, B.E., Keleman, P.B., Mazdab, F.Z., Wooden, J.L., Cheadle, M.J., Hanghoj, K., Schwartz, J.J., 2007. Trace element chemistry of zircon from oceanic crust: a method for distinguishing detrital zircon provenance. Geology 35, 643–646.

Hellebrand, E., Möller, A., Whitehouse, M., Cannat, M., 2007. Formation of oceanic zircons. Goldschmidt Conference 2007, Cologne. Geochimica et Cosmochimica Acta (Suppl. 1), A391.

Hoffmann, A.W., 1997. Mantle geochemistry: the message from oceanic volcanism. Nature 385, 219–229.

Hu, X.F., 1999. Origin of diamonds in chromitites of the Luobusa ophiolite, southern Tibet, ChinaMSc Thesis Dalhousie University (151 pp.).

Irvine, T.N., 1977. Origin of chromite layers in the Muskox intrusion and other intrusions: a new interpretation. Geology 5, 273–277.

Jin, Z.M., Wu, Y., Xu, M.J., Fei, Y.W., Robinson, P.T., 2014. How deep is the Tibetan chromitite: experimental study. Abstract, International Workshop on: Ophiolites, Mantle Processes and Related Ore DepositsChinese Academy of Geological Sciences, Beijing.

Katayama, I., Maruyama, S., Parkinson, C.D., Terada, K., Sano, Y., 2001. Ion micro-probe U–Pb zircon geochronology of peak and retrograde stages of ultrahigh-pressure metamorphic rocks from the Kokchetav massif, northern Kazakhstan. Earth and Planetary Science Letters 188, 185–198.

Katayama, I., Muko, A., Iizuka, T., Maruyama, S., Terada, K., Tsutsumi, Y., Sano, Y., Zhang, R. H., Liou, J.G., 2003. Dating of zircon from Ti-clinohumite-bearing garnet peridotite: Implication for timing of mantle metasomatism. Geology 31, 713–716.

Kelemen, P.B., 1990. Reaction between ultramafic wall rock and fractionating basaltic magma: part I, Phase relations, the origin of calc-alkaline magma series, and the formation of discordant dunite. Journal of Petrology 31, 51–98.

Kelemen, P.B., Dick, H.J.B., Quick, J.E., 1992. Formation of harzburgite by pervasive melt–rock reaction in the upper mantle. Nature 358, 635–641.

Liu, F.L., Xu, Z.Q., Liou, J.G., Katayama, I., Masago, H., Maruyama, S., Yang, J.S., 2002. Ultrahigh-pressure mineral inclusions in zircons from gneissic core samples of the Chinese Continental Scientific Drilling Site in eastern China. European Journal of Mineralogy 14, 499–512.

Liu, F.L., Xu, Z.Q., Xue, H., 2004. Tracing the protolith, UHP metamorphism, and exhumation ages of orthogneiss from the SW Sulu terrane (eastern China): SHRIMP U–Pb dating of mineral inclusion-bearing zircons. Lithos 78, 411–429.

Liu, F.L., Gerdes, A., Robinson, P.T., Xue, H.H., Ye, J.G., 2007. Zoned zircon from eclogite lenses in marbles from the Dabie–Sulu UHP terrane, China: a clear record of ultra-deep subduction and fast exhumation. Acta Geological Sinica 81, 204–225.

Lönngren, M., Kojonen, K., 2005. Dissolution of chromitite ore for platinum group elements and gold analysis, Ray–Iz ophiolitic complex, Polar Urals. In: Törmänen, T. O., Alapieti, T.T. (Eds.), 10th International Platinum Symposium: 'Platinum-group elements — from Genesis to Beneficiation and Environmental Impact', August 8–11, 2005, Oulu, Finland: Extended Abstracts.

Malpas, J., Robinson, P.T., 1987. Origin and tectonic setting of chromite deposits of the Troodos ophiolite. In: Stowe, C.W. (Ed.), Evolution of Chromite Orefields. Van Nostrand-Reinhold Publishers, New York, pp. 220–227.

Malpas, J., Zhou, M.-F., Robinson, P.T., Reynolds, P.H., 2003. Geochemical and geochronological constraints on the origin and emplacement of the Yarlung-Zangbo ophiolites, southern Tibet. Geological Society London Special Publication 218, 191–206.

Moecher, D.P., Samson, S.D., 2006. Differential zircon fertility of source terranes and natural bias in the detrital zircon record: implications for sedimentary provenance analysis. Earth and Planetary Science Letters 247, 252–266.

Moores, E.M., Vine, F.J., 1971. The Troodos Massif of Cyprus, and other ophiolites as ocean crust: evaluation and implications. Philosophical Transactions of the Royal Society of London. Series A, Mathematical and Physical Sciences 268, 443–467.

Nicolas, A., Boudier, F., 2003. Where ophiolites come from and what they tell us. Geological Society of America, Special Paper 373, 137–152.

Pearce, J.A., 1975. Basalt geochemistry used to investigate past tectonic environments on Cyprus. Tectonophysics 25, 41–67.

Pearce, J.A., 2003. Supra-subduction zone ophiolites: the search for modern analogues. Geological Society of America, Special Paper 373, 269–293.

Pearce, J., Robinson, P.T., 2010. The Troodos ophiolitic complex probably formed in a subduction initiation, slab edge setting. Gondwana Research 18, 60–81.

Peltonen, P., Manttari, I., Huhma, H., Kontinen, A., 2003. Archean zircons from the mantle: the Jormua ophiolite revisited. Geology 31, 645–648.

Pervozhikov, B.V., Alimov, V. Yu, Tsaritsin, Ye.P., Chashchukhin, I.S., Sherstobitova, L.A., 1990. Chrome spinels and chromite ore deposits of the massif. Structure, Evolution and Minerogenesis of the Ray–Iz Ultramafic Massif. The Ural Branch of the Academy of Sciences of the USSR, Sverdlovsk, Russia, pp. 149–194 (in Russian).

Pilot, J., Werner, C.-D., Haubrich, F., Baumann, N., 1998. Paleozoic and Proterozoic zircons from the Mid-Atlantic Ridge. Nature 393, 676–679.

Robinson, P.T., Malpas, J., Xenophontas, C., 2003. The Troodos Massif of Cyprus: its role in the evolution of the ophiolite concept. Geological Society of America Special Papers 373, 295–308.

Robinson, P.T., Bai, W.-J., Malpas, J., Yang, J.-S., Zhou, M.-F., Fang, Q.-S., Hu, X.-F., Cameron, S., Staudigel, H., 2004. Ultra-high pressure minerals in the Luobusa ophiolite, Tibet, and their tectonic implications. Geological Society London Special Publication 226, 247–271.

Robinson, P.T., Yang, J., Zhou, M.-F., Xiong, F., 2013. A new model for the formation of podiform chromitites in ophiolites. Mineralogical Magazine 77, 2072.

Rollinson, H., 2005. Chromite in the mantle section of the Oman ophiolite: a new genetic model. The Island Arc 14, 542–550.

Rollinson, H.R., 2008. The geochemistry of mantle chromitites from the northern part of the Oman ophiolite: inferred parental melt compositions. Contributions to Mineralogy and Petrology 156, 273–288.

Rollinson, H., Adetunji, J., 2013. Mantle podiform chromitites do not form beneath mid-ocean ridges: a case study from the Moho transition zone of the Oman ophiolite. Lithos 177, 314–327.

Saveliev, A.A., Savelieva, G.N., 1977. Ophiolites of the Voykar^Syn'insk massif (Polar Urals). Geotectonics 11, 427–437.

Savelieva, G.N., Suslov, P.V., Larionov, A.N., 2007. Vendian tectono-magmatic events in mantle ophiolitic complexes of the Polar Urals: U–Pb dating of zircon from chromitite. Geotectonics 41, 105–113.

Schmelev, V.R., Meng, F.C., 2013. The nature and age of basic rocks of the Rai–Iz ophiolite massif (Polar Urals). Doklady Earth Sciences 451, 758–761.

Searle, M., Cox, J., 1999. Tectonic setting, origin, and obduction of the Oman ophiolite. Geological Society of America Bulletin 111, 104–122.

Shi, R., Alard, O., Zhi, X., O'Reilly, S.Y., Pearson, N.J., Griffin, W.L., Zhang, M., Chen, X., 2007. Multiple events in the Neo-Tethyan oceanic upper mantle: evidence from Ru-Os-Ir alloys in the Luobusa and Dongqiao ophiolitic podiform chromitites: Tibet. Earth and Planetary Science Letters 261, 33–48.

Shi, R., Griffin, W.L., O'Reilly, S.Y., Huang, Q., Zhang, X., Liu, D., Zhi, X., Xia, Q., Ding, L., 2012. Melt/mantle mixing produces podiform chromite deposits in ophiolites: Implications of Re–Os systematics in the Dongqiao Neo-tethyan ophiolite, northern Tibet. Gondwana Research 21, 194–206.

Song, S., Zhang, L., Niu, Y., Su, L., Jian, P., Liu, D., 2005. Geochronology of diamond-bearing zircons from garnet peridotite in the North Qaidam UHPM belt, northern Tibetan plateau: a record of complex histories from oceanic lithosphere subduction to continental collision. Earth and Planetary Science Letters 234, 99–118.

Stern, R.J., Bloomer, S.H., 1992. Subduction zone infancy: examples from the Eocene Izu–Bonin–Mariana and Jurassic California arcs. Bulletin Geological Society of America 104, 1621–1636.

Stern, R.J., Reagan, M., Ishizuka, O., Ohara, Y., Whattam, S., 2012. To understand subduction initiation, study forearc crust; to understand forearc crust, study ophiolites. Lithosphere 4, 469–483.

Thayer, T.P., 1960. Some critical differences between Alpine-type and stratiform peridotite–gabbro complexes. 21st International Geological Congress Report, pt. 13, pp. 247–259.
Thayer, T.P., 1964. Principal features and origin of podiform chromite deposits, and some observations on the Guleman–Soridag district, Turkey. Economic Geology 59, 1497–1524.
Trumbull, R.B., Yang, J.S., Robinson, P.T., Di Pierro, S., Vennemann, T., Wiedenbeck, M., 2009. The carbon isotope composition of natural SiC (moissanite) from the Earth's mantle: new discoveries from ophiolites. Lithos 113, 612–620.
Van der Hilst, R., 1995. Complex morphology of subducted lithosphere in the mantle beneath the Tonga trench. Nature 374, 154–157.
Williams, I.S., 2001. Response of detrital zircon and monazite, and their U–Pb isotopic systematics, to regional metamorphism, and host-rock partial melting, Cooma Complex, southeastern Australia. Australian Journal of Earth Sciences 48, 557–580.
Xiong, F.H., Yang, J.S., Robinson, P.T., Xu, X.Z., Liu, Z., Li, Y., Liu, F., Chen, S.Y., 2015. Origin of podiform chromitite, a new model based on the Luobusa ophiolite, Tibet. Gondwana Research 27, 525–542 (in this issue).
Xu, X., Yang, J.-S., Chen, S.-Y., Fang, Q.-S., Bai, W.-J., Ba, D.-Z., 2009. Unusual mantle mineral group from chromitite orebody Cr-11 in the Luobusa ophiolite of the Yarlung–Zangbo suture zone, Tibet. Journal of Earth Sciences 10, 284–302.
Xu, X., Yang, J., Ba, D., Guo, G., Robinson, P.T., Li, J., 2011. Petrogenesis of the Kangjinla peridotite in the Luobusa ophiolite, Southern Tibet. Journal of Asian Earth Sciences 42, 553–568.
Yamamoto, S., Komiya, T., Maruyama, S., 2004. Crustal zircons from the podiform chromitites in Luobusa ophiolite, AGU Fall Meeting Abstracts 12/2004.
Yamamoto, H., Yamamoto, S., Kaneko, Y., Terabayashi, M., Komiya, T., Katayama, I., Iizuka, T., 2007. Imbricate structure of the Luobusa ophiolite and surrounding rock units, southern Tibet. Journal of Asian Earth Sciences 29, 296–304.
Yamamoto, S., Komiya, T., Hirose, K., Maruyama, S., 2009. Coesite and clinopyroxene exsolution lamellae in chromites: in-situ ultrahigh-pressure evidence from podiform chromitites in the Luobusa ophiolite, southern Tibet. Lithos 109, 314–322.
Yamamoto, S., Komiya, T., Yamamoto, H., Kaneko, Y., Terabayashi, M., Katayama, I., Iizuka, T., Maruyama, S., Yang, J.S., Kon, Y., Hirata, T., 2013. Recycled crustal zircons from podiform chromitites in the Luobusa ophiolite, southern Tibet. Island Arc 22, 89–103.
Yang, J.-S., Dobrzhinetskaya, L., Bai, W.-J., Fang, Q.-S., Robinson, P.T., Zhang, J.-F., Green II, H.W., 2007. Diamond- and coesite-bearing chromitites from the Luobusa ophiolite, Tibet. Geology 35, 875–878.
Yang, J.S., Robinson, P.T., Xu, X.Z., Dilek, Y., 2014a. Ophiolite-hosted diamond: a new occurrence of diamond documented on Earth. Elements 10, 127–130.
Yang, J.S., Meng, F.C., Chen, S.Y., Bai, W.J., Xu, X.Z., Zhang, Z.M., Robinson, P.T., 2015. Diamond, native elements and metal alloys from chromitite of the Ray–Iz ophiolite of the Polar Urals. Gondwana Research 27, 459–485 (in this issue).
Zhou, M.F., Robinson, P.T., 1994. Hi-Cr and high-Al chromitites, Western China: Relationship to partial melting and melt/rock reaction in the upper mantle. International Geological Review 36, 678–686.
Zhou, M.-F., Robinson, P.T., 1997. Origin and tectonic environment of podiform chromite deposits. Economic Geology 92, 259–262.
Zhou, M.F., Robinson, P.T., Malpas, J., Li, Z.-T., 1996. Podiform chromites in the Luobusa ophiolite (Southern Tibet): implications for melt–rock interaction and chromite segregation in the upper mantle. Journal of Petrology 37, 3–21.
Zhou, M.F., Malpas, J., Robinson, P.T., Reynolds, P.H., 1997. The dynamothermal aureole of the Dongqiao ophiolite (northern Tibet). Canadian Journal of Earth Sciences 34, 59–65.
Zhou, S., Mo, X.-X., Mahoney, J.J., Zhang, S.-Q., Guo, T.-J., Zhao, Z.-D., 2002. Geochronology and Nd and Pb isotope characteristics of gabbro dikes in the Luobusha ophiolite, Tibet. Chinese Science Bulletin 47, 143–146.
Zhou, M.F., Robinson, P.T., Malpas, J., Edwards, S.J., Qi, L., 2005. REE and PGE geochemical constraints on the formation of dunites in the Luobusa ophiolite, southern Tibet. Journal of Petrology 46, 615–639.
Zhou, M.F., Robinson, P.T., Su, B.X., Gao, J.-F., Li, J.-W., Yang, J.S., Malpas, J., 2014. Compositions of chromite, associated minerals, and parental magmas of podiform chromite deposits: the role of slab contamination of asthenospheric melts in SSZ environments. Gondwana Research 26, 262–283.